energies

MDPI

Article

Chemically Influenced Self-Preservation Kinetics of CH_4 Hydrates below the Sub-Zero Temperature

Jyoti Shanker Pandey *, Saad Khan and Nicolas von Solms

Center for Energy Resource Engineering (CERE), Department of Chemical Engineering, Technical University of Denmark, 2800 Kongens Lyngby, Denmark; saad_khan_11@hotmail.com (S.K.); nvs@kt.dtu.dk (N.v.S.)
* Correspondence: jyshp@kt.dtu.dk

Abstract: The self-preservation property of CH_4 hydrates is beneficial for the transportation and storage of natural gas in the form of gas hydrates. Few studies have been conducted on the effects of chemicals (kinetic and thermodynamic promoters) on the self-preservation properties of CH_4 hydrates, and most of the available literature is limited to pure water. The novelty of this work is that we have studied and compared the kinetics of CH_4 hydrate formation in the presence of amino acids (hydrophobic and hydrophilic) when the temperature dropped below 0 °C. Furthermore, we also investigated the self-preservation of CH_4 hydrate in the presence of amino acids. The main results are: (1) At T < 0 °C, the formation kinetics and the total gas uptake improved in the presence of histidine (hydrophilic) at concentrations greater than 3000 ppm, but no significant change was observed for methionine (hydrophobic), confirming the improvement in the formation kinetics (for hydrophilic amino acids) due to increased subcooling; (2) At T = −2 °C, the presence of amino acids improved the metastability of CH_4 hydrate. Increasing the concentration from 3000 to 20,000 ppm enhanced the metastability of CH_4 hydrate; (3) Metastability was stronger in the presence of methionine compared to histidine; (4) This study provides experimental evidence for the use of amino acids as CH_4 hydrate stabilizers for the storage and transportation of natural gas due to faster formation kinetics, no foam during dissociation, and stronger self-preservation.

Keywords: formation; dissociation; amino acids; green chemicals; gas uptake; self-preservation

Citation: Pandey, J.S.; Khan, S.; von Solms, N. Chemically Influenced Self-Preservation Kinetics of CH_4 Hydrates below the Sub-Zero Temperature. *Energies* **2021**, *14*, 6765. https://doi.org/10.3390/en14206765

Academic Editor: Jean Vaunat

Received: 24 July 2021
Accepted: 12 October 2021
Published: 17 October 2021

1. Introduction

Natural gas continues to play an essential role in meeting the ever-increasing global demand for energy. Natural gas consumption is expected to increase by 1.3% from the 2019 level, led by the industrial and construction sectors and countries such as China and India [1]. To meet the ever-increasing demand, scientists have started exploring unconventional resources such as shale gas, hydrates, and coal seam gas to secure gas supply. With the increasing demand from developing countries and unconventional sources, long-term efficient, safe, environmentally friendly, and sustainable transportation and natural gas storage are becoming increasingly important. Technologies, such as CNG and LNG, seem to be suitable for long-distance transportation. However, these technologies have problems, such as the extremely low temperature (111 K) required for storage and transportation, leakage due to vaporization, explosiveness due to high pressure, and high operating and safety costs. Therefore, hydrate-based natural gas storage (solidified natural gas–SNG) is considered to be the environmentally friendly technology of the future. In SNG technology, hydrates are stored at moderate pressure and temperatures below the water freezing point in the form of hydrates. In this technology, water and natural gas are mixed to form a crystalline hydrate phase. Because these hydrates melt slowly, they are easier to store and transport compared to earlier technologies.

The kinetics of CH_4 hydrate formation and self-preservation is an important research area for hydrate-based gas technologies such as natural gas storage and transportation [2,3],

CH_4 recovery from hydrate reservoirs [4–8] and CH_4-CO_2 replacement [9]. Information on rapid formation, high storage capacity, and dissociation behavior is essential for the success of these technologies. Laboratory studies show that hydrate formation begins at the gas–liquid interface and that the hydrate formation process is probabilistic, with hydrate growth slowing over time because of the hydrate film-based gas–liquid mass transfer barrier. Mechanical techniques, such as agitation [6] and spraying through the nozzle [10], improve the formation and growth process, but increase power consumption and maintenance complexity. Chemical enhancement involves the application of chemicals, including thermodynamic promoters [11] and kinetic promoters [12,13], to enhance mass transfer under moderate pressure and temperature conditions without mechanical agitation. Due to the self-preservation ability of the CH_4 gas hydrate, it is possible to store solidified natural gas (SNG) long-term at temperatures below freezing. For example, the natural gas hydrate is stored at atmospheric pressure and T = 253 K for three months using the palletization technique [14]. To improve the self-preservation of CH_4 hydrate in different systems, scientists have also tested the self-preservation of CH_4 hydrate in the presence of surfactants [15], hydrophilic silica bed [16], dry water [17], saline water [18,19] and amino acids [20,21]. The effects of amino acids on the enhancement of self-preservation are of particular interest because they are considered an essential component of hydrate-based natural gas storage and transport technology. While it is not yet clear how and why self-preservation improves in the presence of amino acids, this could be the subject of further investigation. The current theory is that the metastability of CH_4 hydrates could be due to the formation of a solid-like layer as a function of temperature at the hydrate interface, which would provide a barrier to heat and mass transfer for the diffusion of gas molecules from the hydrates [22].

Among the kinetic promoters, the anionic surfactant SDS is particularly useful in enhancing hydrate formation and is being studied extensively in detail on a laboratory scale. Critical parameters such as the Kraft point [23] and the critical micelle concentration (CMC) [23] are proposed to understand the correlation between surfactant concentration, solubility, and surface tension. Under hydrate formation conditions, no change in the kraft point is observed; therefore, CMC is used as a reporting parameter in hydrate formation studies [24]. Previous studies show that below the CMC of SDS, absorption and surface tension decrease, while above the CMC, absorption increases, although surface tension remains constant [25].

Amino acids are considered environmentally friendly chemicals that are used in the gas hydrate industry. Laboratory studies have shown that amino acids can act as promoters and inhibitors [26,27]. However, their proper application and the underlying mechanism are not well understood [26,28]. In general, amino acids can be classified into hydrophobic and hydrophilic groups, and their hydrophobic character can be classified by hydropathy indices [29]. The hydropathy of amino acids differs according to their structures and the polarity of their side chain [29]. In this study, two amino acids, L-methionine and L-histidine, are used. L-histidine has a hydrophilic side chain, whereas L-methionine has a hydrophobic side chain. Recent research has shown a relationship between hydrophobicity and hydrate promotion abilities at low concentrations (500–3000 ppm) [30]. Inhibition or promotion in the presence of amino acids is related to their ability to perturb liquid water structure [31], which correlates with hydrophobicity [32]. Some studies confirm that amino acids show a thermodynamic inhibition effect at higher concentrations, which decreases with increasing hydrophobicity [31,33]. The inhibition effect in the presence of amino acids depends on the history of water, the concentration of the additive, and the length and type of amino acid side chains [34].

In this study, methionine and histidine are selected from the hydrophilic and hydrophobic groups to understand the correlation between the concentration and performance of amino acids. Different results are reported in the literature on the performance of hydrophobic and hydrophilic amino acids. For example, histidine behaves as a kinetic hydrate promoter (KHP) in the formation of CH_4 hydrates at 0.03–1 mol% [35] or 0.5 wt% [36].

It also acts as a kinetic hydrate inhibitor (KHI) at 0.1–1 mol% [37]. Similarly, studies show that methionine acts as a KHP at a concentration of 0.5 wt% [28,36]. No experimental observations were made at higher concentration. Studies in the current literature do not include the effects of amino acid concentrations (3000 to 20,000 ppm) above and below 0 °C on the kinetics of CH_4 hydrate formation. Previous studies suggest that hydrophobic amino acids behave as promoters and hydrophilic amino acids behave as KHI when tested at T > 0 °C at a low concentration (3000 ppm), hydrophobic amino acids behave as promoters, and hydrophilic amino acids act as KHI when tested at T > 0 °C [30]. Hydrophobic indices can classify amino acids as promoters or inhibitors at a lower concentration and T > 0 °C. No such comparison is available for T < 0 °C and concentrations greater than 3000 ppm.

Understanding the dissociation behavior of CH_4 hydrates at T < 0 °C in the presence of an additive is critical for the storage and transport of natural gas storage and transportation [38]. Some gas hydrates, such as the CH_4 gas hydrate, dissociate much more slowly at T < 0 °C than at T > 0 °C and this property is called self-preservation. The self-preservation properties of CH_4 gas hydrate are valuable properties that could be useful in gas storage and transportation as gas hydrate under moderate pressure and temperature conditions. Self-preservation is said to depend on guest molecules, co-guest molecules, additives, and grain size of hydrates [39]. Previous studies show that individual self-preservation is observed at temperatures between 240 K and 272 K and is present due to hydrate metastability, additional kinetic barrier, ice layer formation, and secondary hydrate layer [6,40].

Recently, studies have been performed to rapidly form CH_4 hydrate under moderate pressure and temperature conditions using a thermodynamic and kinetic promoter mixture [41]. However, the effect of these chemicals on the self-preservation tendency has not been well investigated. For example, the dissociation of CH_4 hydrates in the presence of an electrolyte (NaCl, $MgCl_2$, Na_2SO_4) was investigated by Sato et al. [18,42] and Mimachi et al. [43]. These studies have shown that electrolyte concentration has a direct effect on hydrate self-preservation such that a higher concentration weakens self-preservation, and a lower concentration improves the self-preservation, and that the tendency of self-preservation of hydrates varies drastically above and below the eutectic temperature. It is necessary to study the effect of additives on the self-preservation tendency since chemically altered self-preservation has not been thoroughly studied. Some existing literature shows the effect of chemicals on self-preservation, such as SDS on CO_2 hydrate formation kinetics [44], and SDS on CH_4 hydrate [15]. Self-preservation is also dependent on the type of guest molecules [39,45]. Another focus is on the kinetics of the formation of CH_4 hydrates in the presence of amino acids when the temperature is lowered below 0 °C.

The kinetics of hydrate nucleation, growth and dissociation are usually explained in terms of the nucleation and dissociation temperature, the onset time, and the total gas uptake profile in a high-pressure cell under stirred and unstirred conditions. Other experimental setups, such as the differential scanning calorimeter (DSC) [46,47], are also used to study the kinetics of CH_4 hydrates. However, the use of rocking cells is limited to the study of kinetic inhibitors and has rarely been used for promotion studies. A rocking cell set-up is a batch reactor consisting of multiple rocking cells within the same temperature bath. All rocking cells follow similar temperature profiles, thus reducing the overall experimental time. Parameters associated with the experimental setup, such as rock angle, rock frequency, solution volume, type of rocking ball material, and operating conditions that affect the performance of the rocking cell, have been studied in detail [48]. Other advantages include the small sample volume and standardization, which facilitates comparing research data between groups [49].

The main objective is to investigate the effect of the concentration of hydrophobic and hydrophilic amino acids on the formation and dissociation kinetics of CH_4 hydrate above and below 0 °C. Different parameters, including onset temperature, induction time, and gas uptake, are investigated using a rocking cell apparatus.

2. Materials and Methods

2.1. Setup and Materials

An analytical grade CH_4 gas cylinder with 99.99% purity is obtained from Air Liquide. Sigma-Aldrich provides L-methionine and L-histidine. L-methionine and L-histidine were selected based on the difference in their hydrophobicity and the availability of supporting literature in our group and elsewhere [21,50] (also see Table A11, Appendix C). L-histidine amino acid is polar and basic, with an aromatic side chain and known to have a moderate promotion effect on hydrate. However, methionine is nonpolar and hydrophobic with an aromatic side chain and exhibits a strong promotion effect on hydrate. Our group has previously tested methionine and histidine using rocking cells for both CH_4 and CO_2/N_2 gas mixtures at constant concentration (3000 ppm) and T > 0 °C [21,30,50,51]. The key conclusion from these studies was that the amino acid promotion ability correlates with their hydrophobicity when tested with a rocking cell. Hydrophobic amino acids methionine showed a stronger promotion ability than hydrophilic amino acids histidine. There are no previous studies investigating the effect of concentration on CH_4 hydrate formation kinetics at T < 0.

A rocking cell setup with five identical high-pressure test cells (RC-5, PSL Systemtechnik, Germany) is used to study changes in amino acid concentration and side chain hydrophobicity on formation and self-preservation kinetics. The rocking cells have five stainless cells immersed in a single liquid bath. Therefore, similar temperatures prevail in all cells at the same time (see Figure 1). The RC-5 bath system can operate up to 200 bar pressure and temperatures ranging from −10 to 60 °C. Measurements for P, T, and temperature can be recorded in the data logging system. The precision of the temperature sensors is in the range of the ±0.2 °C, and that of pressure sensors is in the range of 0.1% [52]. The combined setup uncertainty for the experiments using the Stephanie bell method was calculated to be less than 1% [53]. A detailed discussion of the setup is also provided in our previous articles [54,55]. The Rocking Cell offers additional advantages such as standardization of tests, the possibility of testing at high pressure (up to 200 bar), the ability to run multiple tests simultaneously, and long-lasting stable experiments with accurate measurements that agree with simulation [56]. Distilled water was used to prepare all samples to minimize the influence of impurities in the solution phase. The concentrations ranged from 100 to 20,000 ppm. The experimental details for pure water were taken from our previous publication.

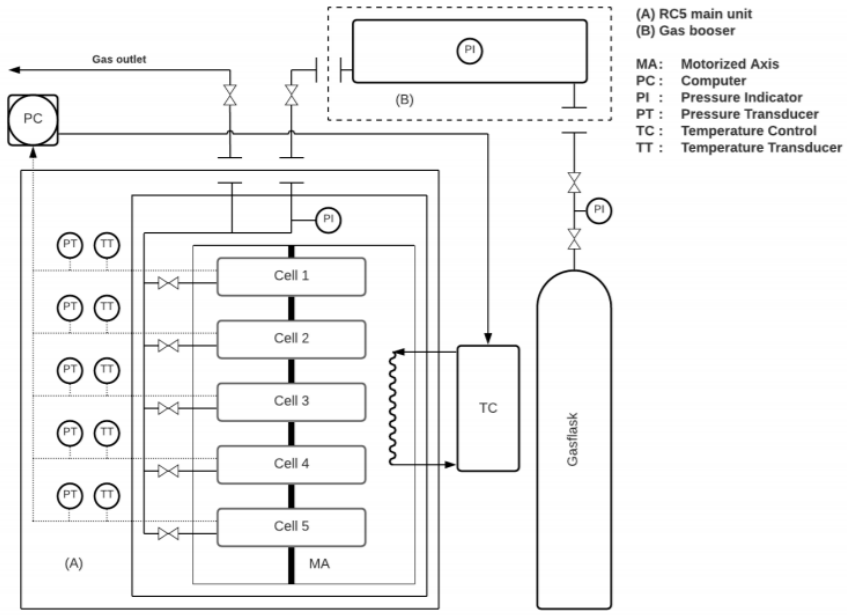

Figure 1. Schematic of rocking cell setup procured from PSL Systemtechnik Germany.

2.2. Procedure and Data Processing

Before starting each experiment, the test cells were cleaned, dried and purged with CH_4 gas to remove any residual air in the system. The total volume in each cell is 40.13 cm^3, and the test volume was 10 cm^3. The rocking rate is 20 bricks/min and the rocking angle is 35°. The system is connected to the data acquisition system during the experiment to record the pressure variations as the temperature in the bath changes. The variation in pressure from 60 bar to 120 bar and temperature varies from −2 °C to 1 °C. Two different temperature programs were selected, the constant ramp program and the isothermal program. The constant ramping and isothermal test procedure is similar to previous studies [57]. The stronger promotion effect also reduces the stochastic nature of hydrate formation; thus, fewer repetitions are needed. Constant ramping experiments are also preferred to isothermal tests to study formation kinetics [48]. Some studies suggest that several hundred repetitions are needed to obtain statistically significant data, the variance in many of the formation kinetic parameters is the function of the driving force [54]. The presence of kinetic promoters enhances the driving force, thus reducing the need for multiple repetitions. The investigation shows a smaller measurement deviation for constant ramp operation than the isothermal experiment. Standard deviation (SD) and margin of error (MOE) were calculated using inbuilt excel functions. These calculations were performed for those experiments in which two trials were carried out. To calculate standard deviation, the stdev command was used. To calculate the margin of error, the T test with a 95% confidence interval was used. Excel command = margin of error (MOE) = Confidence.T(90%, SD, 2).

Constant ramping experiments are carried out at different operating pressures (60–120 bar) according to a predetermined ramping schedule (15–1 °C in 14 h at 1 °C/h) to determine the nucleation temperature (T_0) and the dissociation temperature (T_d) for different concentrations (100–20,000 ppm). T_0 and T_d are determined from the pressure variation curve. The pressure variation during the constant ramp tests is shown in Figures 2–4. The method to calculate T_0 and T_d is been discussed in other publications [57,58]. The temperature of the cells remains in equilibrium with the bath temperature during the experiments. Slow ramping allows the quantification of the degree of supercooling required before hydrate formation begins in the presence of promoters. During constant ramp operation, the initial pressure reduction is due to thermal contraction and gas dissolution in the solution. Pressure and temperature follow a linear trend during the nucleation phase, although a deviation from this linear trend is observed at the beginning of nucleation. Nucleation may have occurred prior to this time, but the deviation from linearity is considered to be the onset of nucleation because of the lack of visual detail. The temperature corresponding to the deviation in the pressure line is considered to be the beginning of nucleation. The point at which nucleation begins is used to calculate the subcooling temperature; see Appendix B for details on data processing. Hydrate formed during the constant ramping experiments was decomposed by heating via ramping. During heating, the temperature in the cell increased linearly as a result of the thermal expansion until the pressure increased as a result of the hydrate decomposition. After hydrate decomposition, pressure again followed a linear trend with temperature.

Isothermal experiments are carried out at constant temperature (1 °C) and at different initial operating pressures (60–120 bar) to record the induction time (to) and CH_4 gas uptake (nCH_4) for different concentrations. Gas uptake kinetics during the isothermal test is influenced by mass transfer, heat transfer and parameters affecting nucleation kinetics. For isothermal experiments, two replicates per experiment (for methionine) were performed, and the values reported are average values. The pressure history curve during the isothermal experiments is shown in Figures 7 and 8. The induction time during our experiment is defined as the time from the onset of rocking to the first significant pressure drop. The standard technique for measuring T_0 and to is described in a previous publication [57].

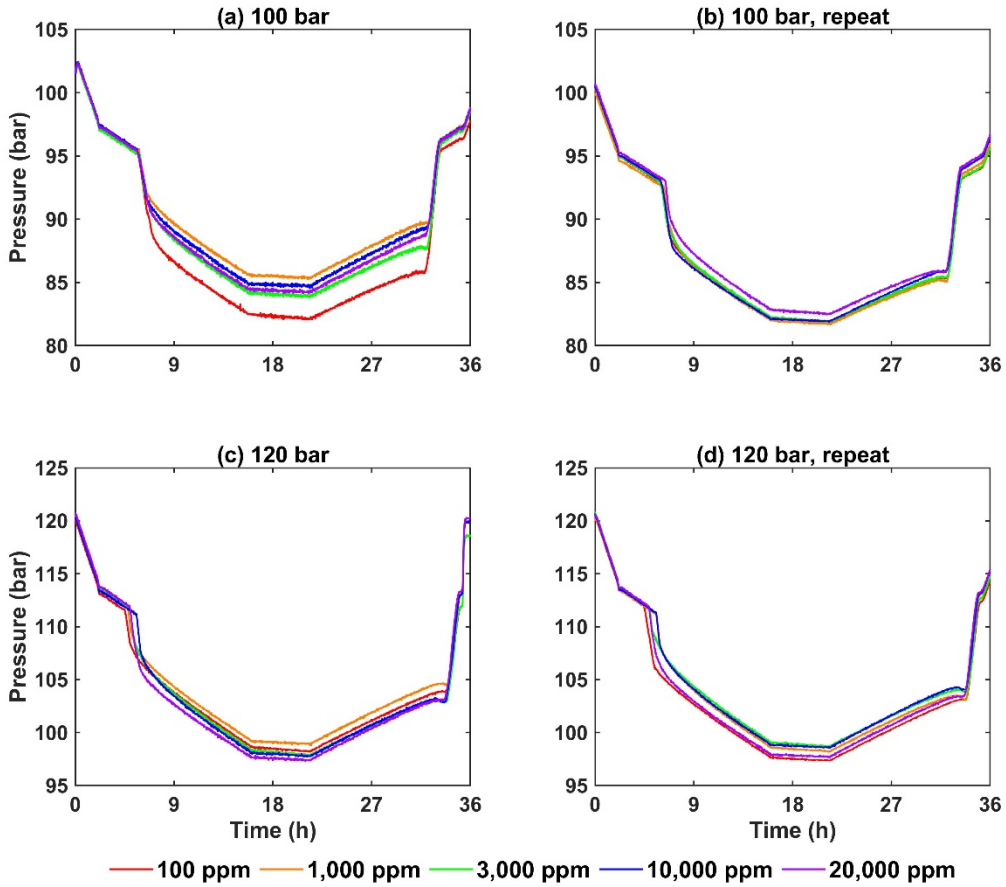

Figure 2. Pressure profiles during the constant ramping temperature scheme in the presence of L-histidine. Starting temperature 25 °C and final temperature 1 °C. Temperature ramping rate 1 °C/h between 15 °C and 1 °C. (**a**) Furthermore, (**b**) show the starting pressure 100 bar (fresh run) and trial 2 (fresh) and (**c**,**d**) the starting pressure 120 bar for trial 1 and trial 2 (fresh), respectively. (**a**) the starting pressure was 102 bar in place of 100 bar.

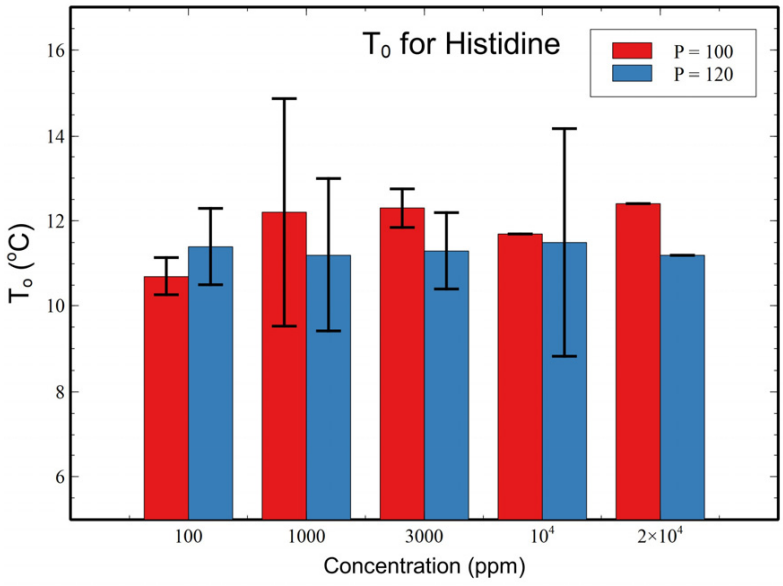

Figure 3. Initial nucleation temperature (T_0) reported for histidine (from constant ramping experiments) at two different initial pressures (100 bar, 120 bar). Margin of error was calculated for 90% confidence interval using t distribution. No margin of error was available for cases with no standard deviation.

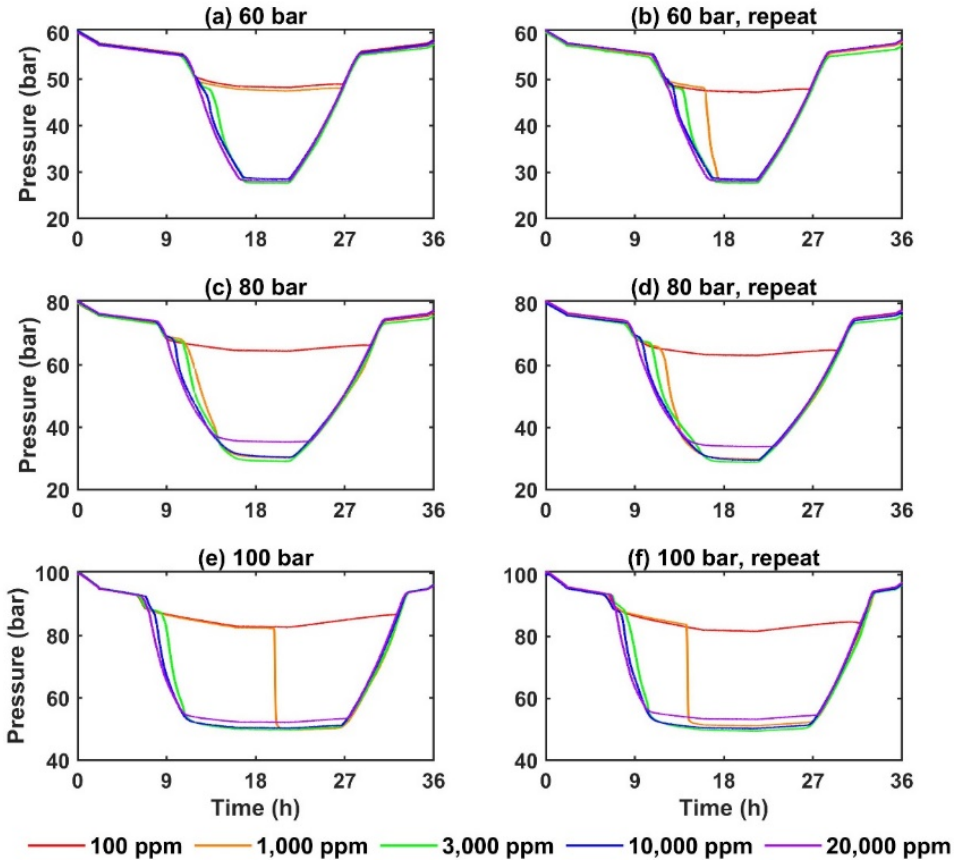

Figure 4. Pressure profiles during the constant ramping temperature scheme in the presence of L-methionine (No memory runs were conducted). Starting temperature 25 °C and final temperature 1 °C. Temperature ramping rate 1 °C/h between 15°–1 °C. (**a**,**b**) show two trials at starting pressure 60 bar and (**c**,**d**) show two trials at starting pressure 80 bar and (**e**,**f**) show two trials at starting pressure 100 bar.

To study CH_4 hydrate self-preservation kinetics, the temperature was reduced from 1 to −2 °C during the isothermal experiment and kept constant at T = −2 °C until the pressure stabilized. Then, degassing was performed rapidly so that the pressure in the cell reached atmospheric pressure; after that, the cell valve was closed and the hydrate began to dissociate as the hydrate pressure was outside the thermodynamic stability zone, and the dissociation was influenced due to the self-preservation property. As the hydrate dissociated, pressure inside the cell continued to increase. Based on the moles of CH_4 released, we measured the ratio of CH_4 (R) (moles of CH_4 release/moles of CH_4 storage in the hydrate). The methodology to measure self-preservation was adopted from the indicated literature [56]. A similar methodology was also used in our previous publication [43]. This study focuses on a qualitative analysis of the influence of L-methionine and L-histidine concentrations on the tendency toward self-preservation of CH_4 hydrate self-preservation. In experiments, many parameters could significantly affect the results but could not be precisely controlled. Therefore, to improve the accuracy of the results, the authors recommend a better experimental design in terms of repeat experiments or a different method. Parameters, such as hydrate saturation, temperature, and impurities in the gas, can affect the self-preservation effect. Several runs should be made for cases with low hydrate saturation.

3. Results

Constant ramp and isothermal temperature schemes are applied to measure the kinetics of formation and dissociation of CH_4 hydrate in terms of the change in concentrations of L-methionine and L-histidine amino acids and driving force (change in concentration,

different initial pressures). The main parameters investigated in the study include the nucleation onset temperature, the dissociation temperature, induction time and the total gas uptake.

3.1. Constant Ramping Experiments

It is common to test kinetic inhibitors using rocking cell setups, and testing low-dose dosage promoters using rocking cells is a more recent practice [57]. Although at least 2–3 replicates are performed in the presence of kinetic inhibitors to account for the stochastic nature of hydrate formation, this may not be necessary for the presence of promoters, as their presence decreases the stochastic nature of hydrate formation. The values reported here are average values from two repeat experiments. The T_0 value is given when a sudden drastic change in the slope of the pressure-time curve is observed. T_0 is often lower in promoters than in pure water [57], suggesting that nucleation in the presence of promoters begins at a lower temperature than in pure water. T_0 is also affected by changes in pressure and concentration, as well as differences in the chemical structure and properties of the chemical compound present in water. Pure water tests were not performed, and the T_0 value for pure water was taken from our previous publications and pressure values from 120 bar to 50 bar [57]. Details are given in Appendix A Table A1.

Constant ramp experiments for the formation of CH_4 hydrates in the presence of histidine were performed at 100 bar and 120 bar. Figure 2 shows the pressure profile for the first and repeat runs for fresh samples for histidine. No memory runs were performed. Table A1 in Appendix A summarizes the T_0 values along with the margin of error calculated for histidine at five different concentrations (100 to 20,000 ppm). Figure 3 shows the graphical representation of the data in Table A2.

For histidine, T_0 at a very dilute concentration (100 ppm) decreases from 11.4 °C to 10.7 °C when the pressure increases from 100 bar to 120 bar. However, at a concentration of 1000 ppm and above, T_0 increased when the pressure increased from 100 bar to 120 bar. For example, T_0 increased from 11.2 to 12.2 °C (1000 ppm) and from 11.2 °C to 12.4 °C (20,000 ppm). This was consistent with the general observation for pure water (see Appendix A). Typically, the presence of histidine in the water lowered the T_0 value compared to pure water, indicating a delay in the onset of nucleation due to the higher driving force requirement. For a given initial pressure and an increase in concentration from 100 ppm to 20,000 ppm, T_0 increased from 10.7 to 12.4 °C (at 120 bar). This observation suggests that a lower driving force is required for a higher concentration and that a higher concentration has the advantage that nucleation starts earlier. The effect of concentration on T_0 was more pronounced at 120 bar than at 100 bar in histidine, as no hydrate formation was observed at 100 bar pressure.

Figure 4 shows the pressure curve for five different concentrations of methionine at 60–100 bar. Table A3 in Appendix A summarizes the T_0 temperatures calculated for methionine. T_0 increases for all concentrations as the pressure increases from 60 bar to 100 bar.

At a given starting pressure P = 100 bar, methionine had a lower T_0 compared to histidine. (10.7–11.1 °C for methionine, 11.2–11.4 °C for histidine). When the methionine concentration increased from 100 ppm to 20,000 ppm, T_0 changed from 11.1 to 10.7 °C at P = 100 bar. This indicates that the increase in methionine concentration delayed nucleation and that a higher level of supercooling was required for the onset of nucleation. The correlation between concentration and T_0 was the same for P = 100 bar to 60 bar. The influence of concentration on T_0 was more evident at higher pressure than at lower pressure.

The experimental study suggests that $T_0 < T_{eq}$ (water) (refer to Tables A1–A3 in Appendix A) for both histidine and methionine, indicating delayed nucleation in the presence of amino acids and a higher supercooling requirement compared to the case of pure water. T_0 was lower for methionine compared to histidine at a given pressure. For both histidine and methionine, T_0 increases with pressure, implying that the subcooling requirement decreases with increasing pressure, and the effect of concentration on T_0 was more evident at higher pressure. The effect of concentration on T_0 was different for histidine and methionine. At 100 ppm ultralow concentration, T_0 = 11.1 °C (methionine)

was less than 11.4 °C (for histidine), suggesting a more substantial effect of methionine on the subcooling requirement even at lower concentration.

Figure 5 shows the data from Tables A2 and A3 (Appendix A) graphically. T_0 is compared only for methionine and histidine at 100 bar. The effect of concentration on T_0 is visible at 120 bar for histidine (see Figure 3). Comparison of T_0 for histidine and methionine at P = 100 bar shows that T_0 is higher for histidine than for methionine at all concentrations, indicating lower supercooling requirements for histidine than for methionine at P = 100 bar. Histidine consists of a carboxyl group and an amine group, which facilitates hydrogen bonding with water molecules. Amino acids tend to behave as zwitterions, which results in a strong electrostatic interaction between the electric charges on the amino acids and the water molecules, which disrupts the structure of the water cages of the hydrates. However, some amino acids, such as glycine, similar to histidine, were shown not to affect the structure of CH_4 hydrate when a powder X-ray diffraction experiment was performed [59]. Different supercooling requirements for different concentrations of a particular chemical indicate different operating requirements to initiate hydrate formation. High subcooling indicates that a significant pressure drop below the equilibrium pressure is required to initiate nucleation. MOE was higher for 100 bar.

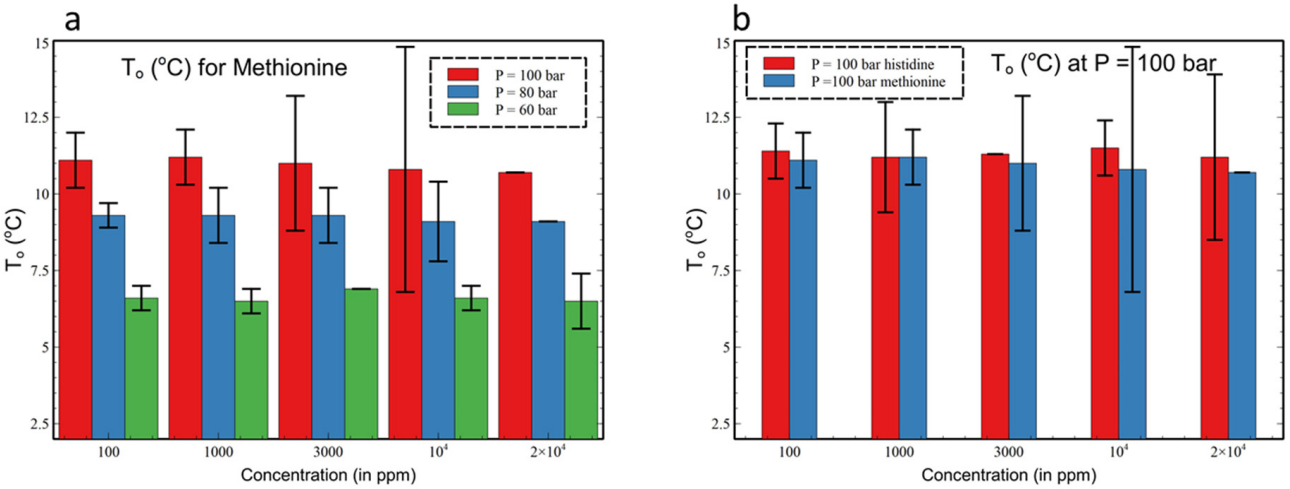

Figure 5. Initial nucleation temperature (T_0) calculated from the constant ramping temperature scheme in the presence of L-histidine and L-methionine for different concentrations for a fresh run. (**a**) Onset temperature variation for L-methionine for different concentration at P = 60, 80 and 100 bar. (**b**) T_0 variation at 100 bar for histidine and methionine. Margin of error was calculated for 90% confidence interval using t distribution.

In general, the effect of concentration on T_0 at higher pressure (100 bar or more) was observed for both amino acids. Due to the slight change in concentration from 100 ppm to 20,000 ppm (2 wt.%), the variations in T_0 were not very large, but high concentrations were avoided due to possible inhibition, as observed in other studies. For example, when histidine was used at a concentration of 0.5–1.5 wt.% for the C_2H_6 gas, it behaved as a kinetic inhibitor [60]. In another study, histidine behaved as an inhibitor when used at 1% by weight for the CH_4 + C_3H_8 mixture [61]. Another critical factor in the evaluation of the kinetics is the design of the experimental setup. Histidine has been shown to behave as a kinetic promoter when used in a stirred reactor at 1 °C and 50 bar pressure at a concentration of 1 wt.% [37]

3.2. The Onset of the Dissociation Temperature (T_d)

Constant ramping experiments were also performed to measure the onset of the dissociation temperature during slow heating (1 °C/h). Table A4 in Appendix A shows the averaged T_d value for histidine and methionine at five different concentrations. The variation of T_d with concentration under different pressures is shown in Figure 6.

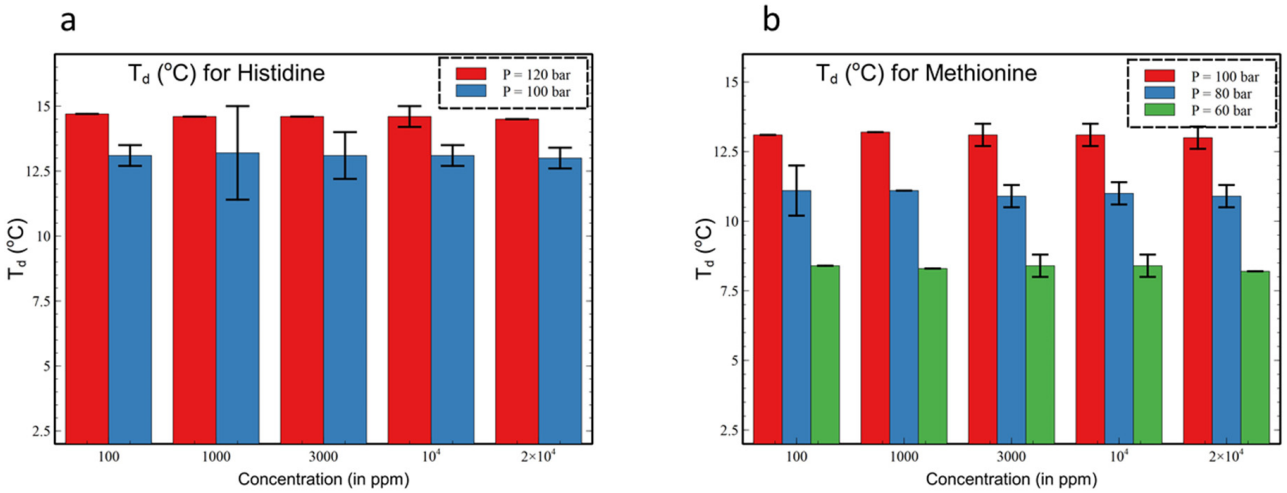

Figure 6. Dissociation temperature (T_d) during an isothermal experiment at 1 °C (for histidine and methionine) at five different concentrations (100 ppm to 20,000 ppm). (**a**) Dissociation temperature T_d for histidine under two different starting pressures (100 and 120 bar.) (**b**) Dissociation temperature T_d for methionine under three different starting pressures (60 bar, 80 bar and 100 bar).

An increase in starting pressure causes an increase in T_d at a given concentration. This suggests that the stability of the hydrate increases with increasing starting pressure. For example, at 3000 ppm methionine, an increase in starting pressure from 60 bar to 100 bar increases T_d from 8.4 °C to 13.1 °C. Similarly, for histidine, when the pressure increases from 100 bar to 120 bar, T_d increases from 13.1 °C to 14.6 °C. Furthermore, the change in concentration has little effect on T_d. For example, the T_d for methionine at 100 bar remains between 13.0 and 13.2 °C when the concentration increases from 100 ppm to 20,000 ppm. Similarly, at 60 bar, T_d remains between 8.2 and 8.4 °C. The situation is similar for histidine. T_d is similar for histidine and methionine at P = 100 bar, suggesting that T_d is independent of the presence of chemicals but dependent on the starting pressure. A review of the literature on the effect of amino acids on the dissociation behavior of hydrates shows that increasing amino acid concentration leads to a slight improvement in the gas release rate when it is above 0 °C [35].

3.3. Induction Time

To measure induction time and total gas uptake, isothermal experiments are performed at 1 °C in the presence of histidine and methionine; Induction time results are summarized in Table A5 in Appendix A. Cases in which rapid hydrate formation did not occur are indicated by NH. The induction [62] time during the memory run is generally shorter due to the memory effect of water. The induction time is the time difference between the gas injection and immediately before the rapid pressure drop. Knowledge of the induction time during the hydrate formation phase is essential for selecting the appropriate promoter with the optimum concentration. In isothermal experiments, the difference in the driving force is the difference in pressure between the initial injection pressure P1 and P_{eq}. P_{eq} is calculated at a constant temperature using CSMGem software [63]. For isothermal experiments, P_{eq} = 28.5 bar for the CH_4 gas hydrate at T = 1 °C. Therefore, an increase in the initial pressure increases the driving force in hydrate formation.

Figure 7 shows the pressure profiles at the initial pressure of 100 bar and 120 bar during the isothermal experiment for fresh and memory runs in the presence of histidine. The change in concentration from 100 to 20,000 ppm during the pressure run is recorded to measure the induction time and the total molar content of CH_4 in the gas hydrate. Figure 6 shows no rapid pressure drop in the presence of histidine at all concentrations and an initial pressure of 100 bar. However, a rapid pressure drop was observed at operating

pressures of 120 bar for concentrations of 3000 ppm and higher. In histidine, no further experiments were carried out as sufficient historical data was not available.

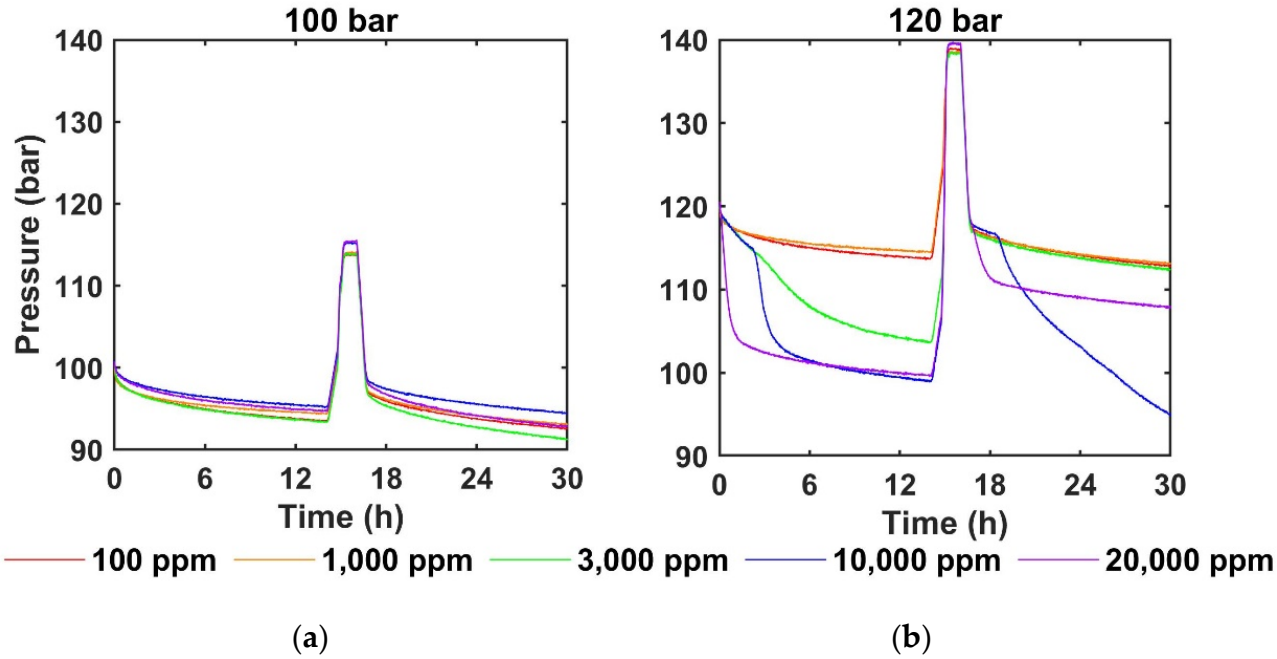

Figure 7. Pressure variation (for fresh and memory run) during the isothermal experiment temperature (T = 1 °C) scheme (in the presence of L-histidine) at five different concentrations (100 ppm to 20,000 ppm) for two different pressures (100 bar and 120 bar). (**a**) Pressure profiles during isothermal under 100 initial bar pressure (no rapid pressure drops observed) and (**b**) pressure profiles during an isothermal experiment under 120 initial bar pressure. (Rapid pressure drops observed for 3000 ppm concentration and above).

In our previous work, we compared the different amino acids at a concentration of 3000 ppm to form CH_4 hydrate using a rocking cell [41]. In that study, we found a total pressure drop of 5.5 bar (fresh) and 4.3 bar (memory) during isothermal cooling at P = 100 bar, T = 1 °C. In the current experiment, a total pressure drop of 6.9 bar (fresh) and 5.5 bar (memory) was found (see Table A5 in Appendix A).

Figure 8 shows the pressure profiles (two trials) during the isothermal experiment for fresh and memory runs in the presence of methionine. The change in concertation from 100 to 20,000 ppm in the pressure response is recorded to measure the induction time and the total mol of CH_4 in the gas hydrate.

The induction time for methionine is shorter than that for histidine because of the strong perturbation of hydrogen bonding between the water molecules that results from an increase in the initial operating pressure and an increase in concentration. In the presence of histidine, no rapid pressure drop is observed at all concentrations when the initial operating pressure is 100 bar. When the pressure increases from 100 bar to 120 bar, rapid hydrate formation is observed at a concentration of 3000 ppm and above. For methionine, the induction time is reduced by 3 min for both the fresh and the memory run (P = 60 bar − 100 bar, T = 1 °C). In our previous study, the total pressure drop was 41 bar (fresh) and 40 bar (memory) [50], while in the current study, the total pressure drop was 36 bar (fresh) and 34.5 bar (memory) (see Table A6 in Appendix A).

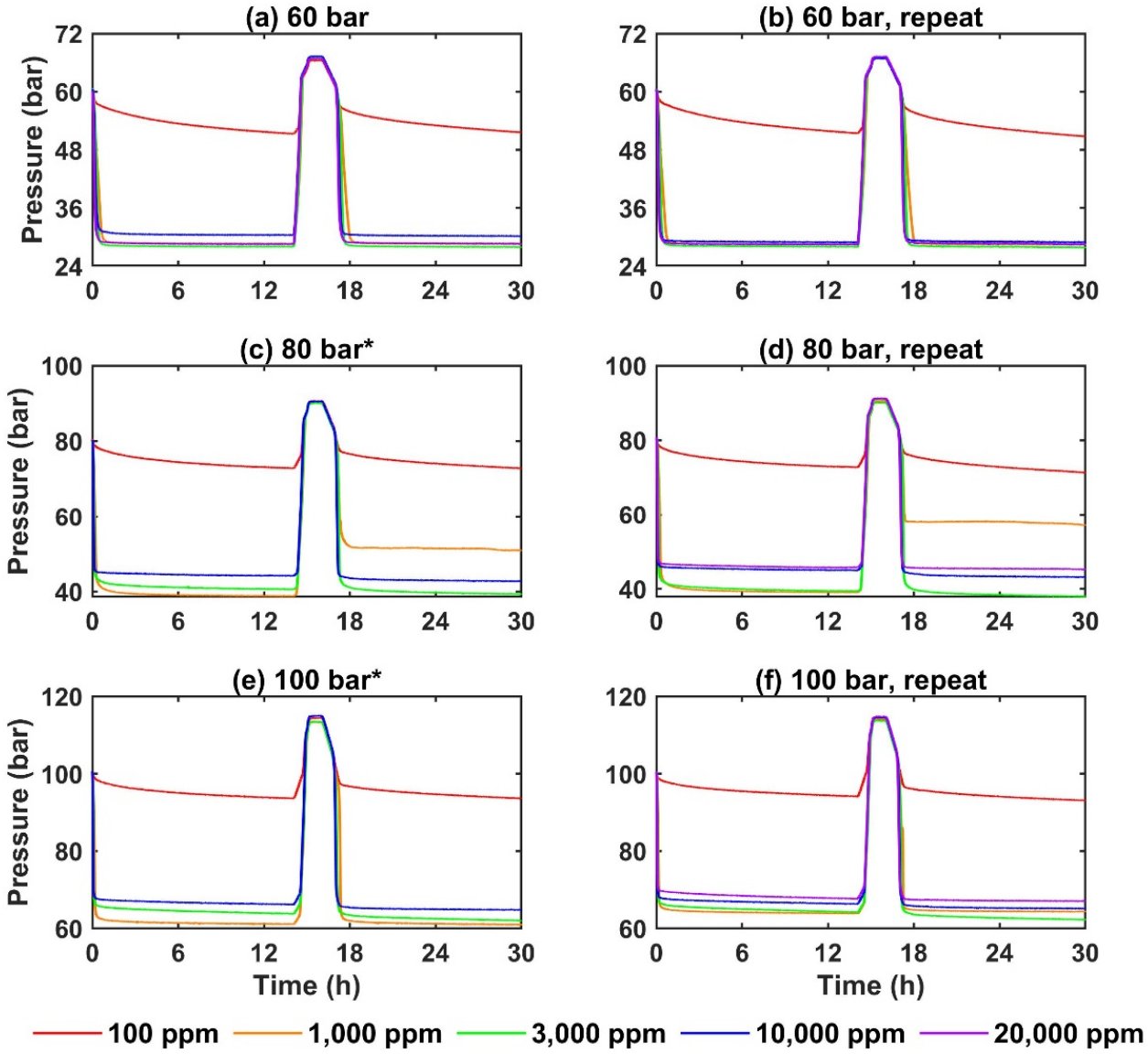

Figure 8. Pressure variation (for fresh and memory run) during the isothermal experiment temperature (T = 1 °C) scheme (in the presence of L-methionine) at five different concentrations (100 ppm to 20,000 ppm) for three different pressures (60, 80 and 100 bar). (**a**,**b**) show pressure profiles during isothermal under 60 bar initial pressure; (**c**,**d**) shows pressure profiles during an isothermal experiment under 80 bar initial pressure. (**e**,**f**) shows pressure profiles during an isothermal experiment under 100 bar initial pressure.

3.4. Total Gas Uptake above 0 °C

Total gas uptake was calculated (calculation methodology explained in Appendix B) using an isothermal experiment at T = 1 °C and P1 = 100 bar and 120 bar for L-histidine and P1 = 60, 80 and 100 bar for L-methionine. Table A6 in Appendix A summarizes the total uptake of CH_4 gas in hydrates in the presence of histidine at five different concentrations, and the results are shown graphically in Figure 9. The experimental analysis shows no rapid growth during the formation of hydrates at P = 100 bar (refer to Figure 7). Increasing the histidine concentration does not cause any rapid pressure drop and no change in total stored gas, and most of the stored gas could be due to loss of CH_4 due to solubility in water. No rapid pressure drop was observed in the fresh and memory run at P = 100 bar (for histidine). This observation differs from previous studies (Table A11 in Appendix C) due to the different experimental setup, which may result in a different gas/liquid contact area as well as a different agitation mechanism. Other experiments

were also run at constant pressure, while our experiments were run at constant volume, where the driving force continued to decrease with the hydrate formation process. When the pressure increased from 100 bar to 120 bar, rapid hydrate formation was observed at concentrations of 3000 ppm and higher. Maximum gas uptake is observed at 10,000 ppm. Another observation concerned the difference in total gas uptake between fresh and memory runs. The total gas uptake during the memory run was found to be less than that during the fresh run. Therefore, parameters such as initial operation pressure (P1 = 120 bar) and concentration (3000 ppm and above) influence CH_4 hydrate formation ability and driving forces in the presence of histidine. The temperature of hydrate formation, the reactor design and the degree of mechanical agitation should also be considered as influencing variables, as our observation differed from previous studies [37]. No repeated experiments were performed for 100 bar or 120 bar.

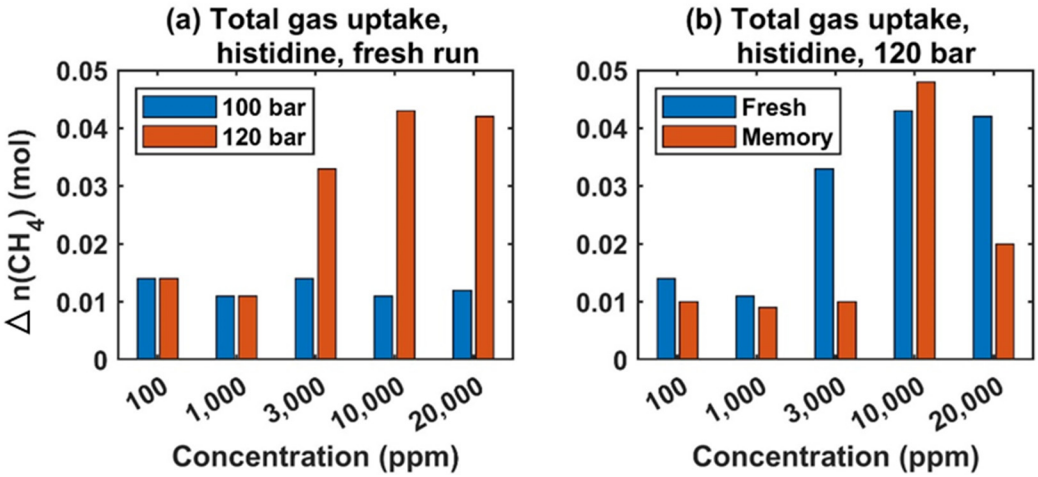

Figure 9. Total CH_4 uptake during the isothermal experiment at 1 °C for histidine at different concentrations. (**a**) Total gas uptake profiles for different concentrations under 100 bar and 120 bar. (**b**) Total gas uptake variation for different concentrations under 120 bar for fresh and memory run.

Similarly, Table A7 in Appendix A summarizes the total uptake of CH_4 gas in hydrates in the presence of L-methionine at five different concentrations. The values reported are based on the average of two runs for both the fresh and the memory runs (see Figure 8). During the isothermal temperature scheme, the pressure variation shows a rapid pressure drop at a methionine concentration of 1000 ppm and above. At a concentration of 100 ppm, the change in pressure from 60 bar to 100 bar did not increase the total gas uptake and total pressure drop. At a concentration of 1000 ppm and above, the effect of pressure on gas uptake was visible. A drastic increase in gas uptake was observed between 100 and 1000 ppm, which improved further with increasing concentration up to 3000 ppm. The optimum gas uptake was observed at a concentration between 3000 and 10,000 ppm. At a concentration of 10,000 ppm and above, the total gas uptake was reduced, suggesting that the short induction time at high chemical concentration caused a lower gas–liquid contact time, thus decreasing the amount of gas trapped in the hydrates. As pressure increased from 80 bar to 100 bar, did not result in a substantial increase in gas uptake. Therefore, total gas uptake was measured in the pressure range of 80–100 bar. Figure 10 illustrates the data from Table A7. The Margin of Error (ME) calculation shows that higher values were recorded when the driving force was low (lower concentration, lower pressure). Higher ME values are also indicative of weaker promotion abilities and a higher stochastic nature, so additional experimental work is required in such cases.

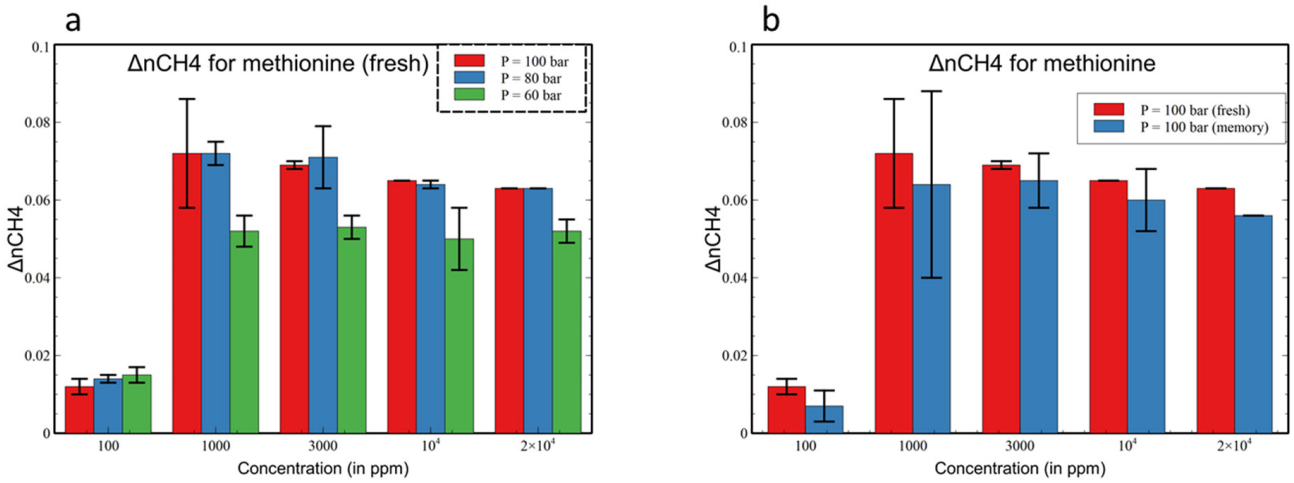

Figure 10. Total CH_4 uptake during an isothermal experiment at 1 °C for methionine at different concentrations. (**a**) Total gas uptake profiles for different concentrations under 60 bar, 80 bar and 100 bar. (**b**) Total gas uptake profiles for different concentrations under 100 bar for fresh and memory runs.

For both amino acids, it was observed that the memory solution has a lower gas uptake than the fresh solution (see Figure 9), which raises the question of recycling the saturated amino acid solution. However, the disposal of such a solution after the dissociation cycle would be environmentally friendly. The deviation in total gas uptake between fresh and memory runs decreased with increasing concentration. The minimum deviation was found at a concentration between 3000 and 10,000 ppm. When gas uptake between histidine and methionine was compared, it was found that methionine and histidine did not enhance hydrate formation at a concentration of 100 ppm. At a higher concentration of 1000 ppm and above, a difference in their promotion ability was visible. For example, gas uptake at 100 bar, gas uptake varied between 0.01–0.15 (for histidine) and 0.03–0.04 (for methionine). When comparing the ME value for the fresh and memory run, it was found that the margin of error was consistently higher for the memory run than for the fresh run.

3.5. Self-Preservation Kinetics at T < 0 °C

The pressure profiles in the presence of histidine are shown in Figure 11 when the temperature drops from 1 °C to −2 °C, followed by rapid degassing at T = −2 °C. Data can be found in Table A8 in Appendix A (refer to Figure 12). When the temperature is cooled below 0 °C, a rapid pressure drop is observed for histidine at a concentration greater than 1000 ppm. At a P1= 100 bar, a pressure drop first occurred at 3000 ppm, followed by a pressure drop at 1000 ppm. At 10,000 and 20,000 ppm, a minor pressure drop was also observed. No pressure drop was recorded for the 100 ppm concentration. Total gas uptake in hydrates improved by three to six times due to cooling below 0 °C. The largest increase in moles stored in hydrate was observed for the concentration range between 1000 ppm and 3000 ppm. Similarly, for the experiment at P1 = 120 bar, rapid pressure drops were observed for concentrations 3000 ppm to 10,000 ppm. Total gas uptake improved by 1.5 to 4.8 times due to cooling below 0 °C. Pressure drops were observed at concentrations between 3000 and 10,000 ppm. Combining the observations at 100 bar and 120 bar, it is found that cooling below 0 °C could improve the formation kinetics and total gas uptake in the presence of a 1000–10,000 ppm concentration of histidine. These results depend on the reactor design and mechanical agitation as a result of the difference in the experimental setup (rocking cell in this case). Cooling below 0 °C provides an additional driving force that accelerates hydrate formation in the presence of histidine, which in our case acts as a weak promoter above 0 °C.

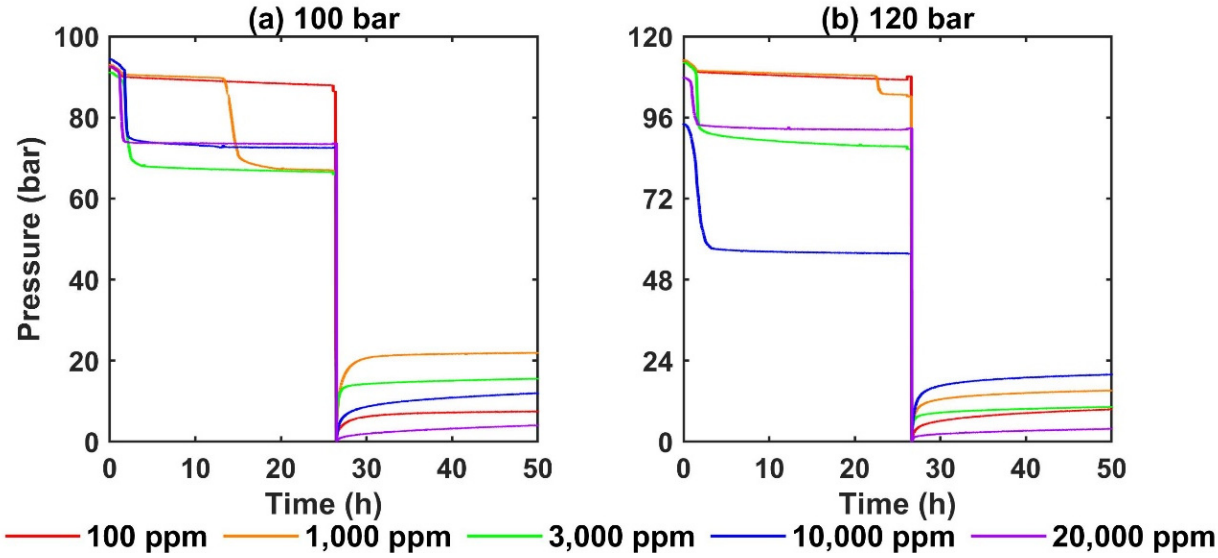

Figure 11. Pressure variation during cooling T < 0 °C in the presence of histidine for different concentrations. First part of pressure variation on account of cooling below 0 °C (temperature reduced from 1 °C to −2 °C) and second part of pressure variation due to self-preservation. For self-preservation, the pressure inside the cells was quickly reduced to atmospheric pressure thereafter valve was closed (at T = −2 °C) (**a**) shows the pressure response curve for P_1 = 100 bar. (**b**) shows the pressure response curve for P_1 = 120 bar.

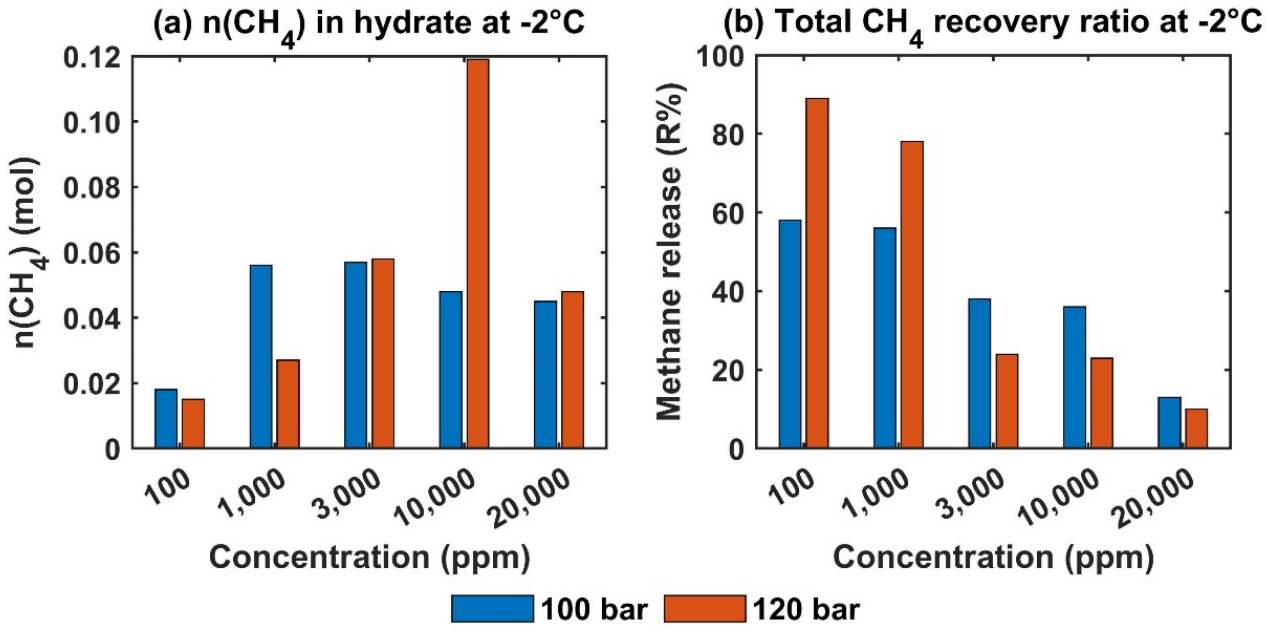

Figure 12. Effect of temperature decrease from 1 °C to −2 °C on the CH_4 uptake in hydrate (in the presence of histidine) (refer (**a**)) for two different starting pressures (100 and 120 bar). (**b**) shows CH_4 (R) number (for five different concentrations of histidine) at two different pressures (100 and 120 bar) at T = −2 °C.

The rate of hydrate dissociation is much slower at T < 0 °C than at T > 0 °C because of the self-preservation of CH_4 hydrate. Previous studies show that increasing hydrate saturation decreases self-preservation due to lower ice saturation on the hydrate surface [35]. Furthermore, lowering the temperature and increasing the pressure improve self-preservation and decrease the dissociation of hydrates below 0 °C [36–38]. Experimental measurements show that the presence of histidine affects the rate of hydrate dissociation (self-preservation tendency) of CH_4 hydrates at T = −2 °C (see Table A8 in Appendix A). As histidine concentration increases, the dissociation of CH_4 hydrate is delayed and the

amount of CH_4 release is reduced. CH_4 (R) was defined as the amount of CH_4 released with respect to the amount of CH_4 stored in the hydrates. This was done to normalize the effect of CH_4 stored in hydrates, as different amounts of concentrations caused different CH_4 stored in hydrates before rapid depressurization. The variation in CH_4 (R) at T = −2 °C for different concentrations provides additional information. For example, at a concentration of 3000 ppm–20,000 ppm, CH_4 (R) ranges from 38% to 13% (at P_1 = 100 bar) and from 24% to 10% (at P_1 = 120 bar). The decrease in CH_4 (R) shows lower CH4 released due to stronger self-preservation. For concentrations between 100 ppm and 1000 ppm, CH_4 release (R) varies from 56% to 58% (at P_1 = 100 bar) and from 78% to 89% (at P_1 = 120 bar). The initial increase in CH_4 (R) at a lower concentration suggests that concentration does not influence self-preservation. At a given concentration, the values of CH_4 (R) values are higher for P_1 = 120 bar compared to P_1 = 100 bar due to the higher initial hydrate saturation caused by the high initial pressure. However, for a given initial pressure, increasing the saturation of concentration increases the hydrate saturation and decreases the release of CH_4 at T < 0 °C. (at concentration greater than 3000 ppm) For example, CH_4 (R) decreased from 38% to 24% (at 3000 ppm) and from 13% to 10% (at 20,000 ppm) for histidine. A very low CH_4 (R) number at high concentration indicates high metastability in the presence of histidine. It can be concluded that an increase in the concentration affects the hydrate dissociation ability by promoting hydrate metastability. This indicates the usefulness of histidine (hydrophilic) in water for the stability of CH_4 hydrates at negative temperatures for storage and transportation purposes.

In another experiment, the metastability of CH_4 hydrate was studied in the presence of methionine at P_1 = 60−100 bar. Figure 13 shows the pressure response curves (for methionine) during the self-preservation studies of CH_4 hydrate (at three different starting pressures). The pressure response curve is divided into two parts. The first part of the pressure response curve is due to cooling below subzero when the temperature dropped to T = −2 °C. The second part of the pressure response curve is due to degassing to atmospheric pressure and subsequent hydrate dissociation outside its stability zone but in the presence of self-preservation. The pressure response curve (in the presence of methionine) is different from that of histidine. No significant pressure drop was observed on account of cooling below 0 °C, which was observed in histidine. Therefore, it can be said that maximum hydrate saturation was achieved under conditions of T > 0 °C. The total moles of CH_4 stored in hydrates and released during self-preservation studies at T = −2 °C are summarized in Tables A9 and A10 in Appendix A. The CH_4 (R) value is the normalized fraction of CH_4 molecules released into CH_4 molecules stored in hydrate at T = −2 °C. The higher the CH_4 (R) value, the weaker the self-preservation. Figure 14 illustrates the data (from Table A9 in Appendix A), including the R-value for 60, 80 and 100 bar.

Similar to what was previously observed in the presence of histidine, R (CH_4 release/CH_4 storage in the hydrate) decreased when the methionine concentration (above 3000 ppm) increased at a given pressure. For example, R decreased from 13% to 3% at P_1= 60 bar, from 17% to 6% at P_1 = 80 bar, and from 34% to 7% at P_1= 100 bar. The R value reaches its maximum at a concentration between 1000 and 3000 ppm, after which the R value continues to decrease. The increase in the R value (at low methionine concentration) could be related to the increase in hydrate saturation and the absence of chemical effect on self-preservation. It is known that CH_4 stored in hydrate increases (when the methionine concentration increases), the R value should also increase (high hydrate saturation dissociates faster than low hydrate saturation); however, the R value was lower at high hydrate saturation (according to our observation), suggesting an influence of chemicals on self-preservation (at high methionine concentration). An increase in hydrate saturation decreases ice saturation for a given volume of liquid. At lower concentrations (100 to 3000 ppm), the initial hydrate saturation increases with increasing pressure, but the R value increases. Therefore, the effect of methionine on the metastability of CH_4 hydrates was weaker at lower concentrations and self-preservation was governed by hydrate saturation. For example, R increased from 13% to 34% for 100 ppm when the pressure increased from 60 bar to 100 bar. However, at a

higher concentration of 20,000 ppm, R increased only from 3% to 7%, clearly showing the effects of chemicals on hydrate metastability or self-preservation. In a previous study, the effect of chemical L-methionine on improving the metastability of gas hydrates was also confirmed [53]. However, the mechanism by which amino acids influence the metastability of CH_4 hydrates is not yet understood.

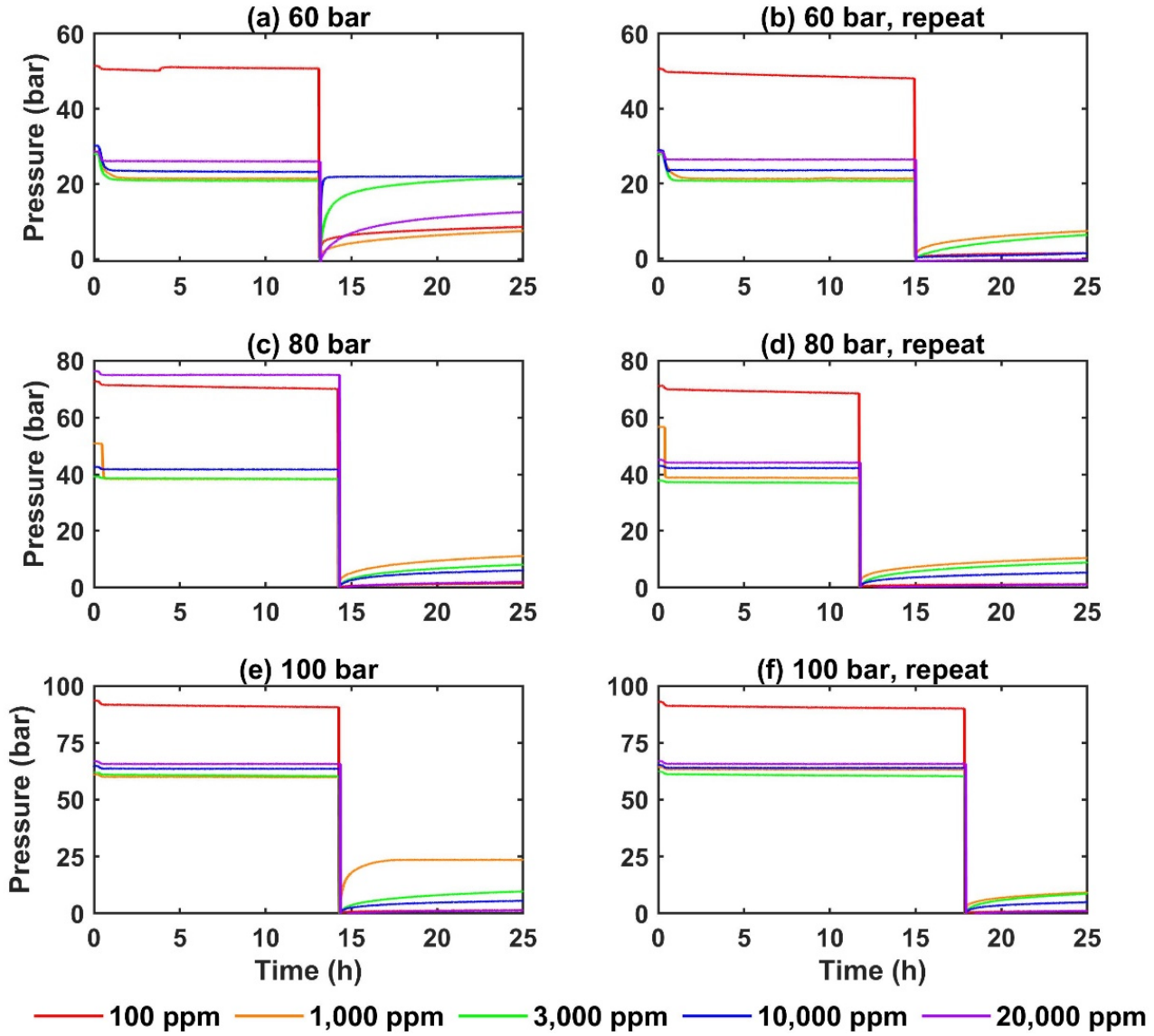

Figure 13. Pressure variation during cooling T < 0 °C (in the presence of methionine) for five different concentrations (100 ppm to 20,000 ppm). First part of pressure variation on account of cooling below 0 °C (temperature reduced from 1 °C to −2 °C) and second part of pressure variation due to self-preservation. For self-preservation, the pressure inside the cells was quickly reduced to atmospheric pressure and valve was closed (at T = −2 °C) (**a**,**b**) show the pressure response curve for P_1 = 60 bar. (**c**,**d**) show the pressure response curve for P_1 = 80 bar. (**e**,**f**) show the pressure response curve for P_1 = 100 bar.

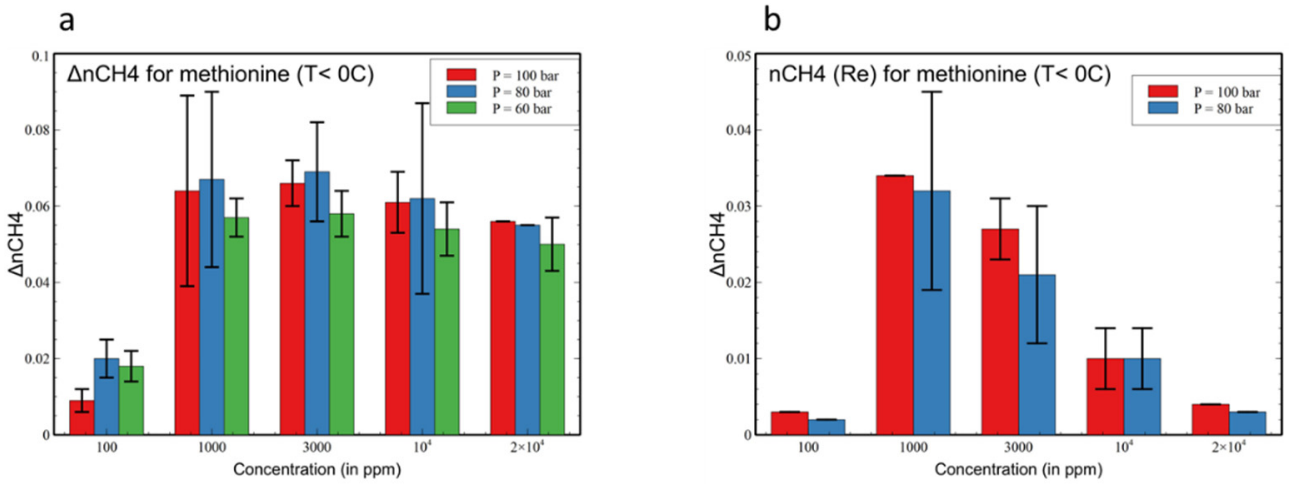

Figure 14. Effect of temperature decrease from 1 °C to −2 °C on the CH_4 uptake in hydrate (in the presence of methionine) (refer (**a**)) for three different starting pressures (60, 80 and 100 bar). (**b**) shows CH_4 (R) number (for five different concentrations of methionine) at three different pressures (60, 80 and 100 bar) at T = −2 °C.

An earlier study compared the dissociation of CH_4 hydrate below 0 °C in the presence of amino acids and SDS at a concentration of 3000 ppm to understand the effects of chemicals on the dissociation behavior. The study concludes that hydrophobic amino acids better retard hydrate dissociation below 0 °C than SDS [21]. In this study, we extend and study the effect of varying the concentration of amino acids on the dissociation rate of CH_4 hydrates at T < 0 °C. For P = 100 bar, the initial moles stored in CH_4 hydrates range from 0.056 to 0.066 (for methionine) and from 0.045 to 0.057 (for histidine) when the concentration varied from 3000 to 20,000. R ranged from 7% to 42% (methionine) and from 13% to 38% (histidine). Typically, for concentrations of 10,000 ppm and 20,000 ppm, the metastability of CH_4 hydrate (based on methionine) was much stronger than that of histidine. (see Tables A7 and A8 in Appendix A). Further investigation should be carried out to compare the other amino acids (with hydrophobic and hydrophilic characteristics) and SDS.

Our study also shows the calculation of the margin of error (ME) in different experiments. ME values were lowest for a higher concentration or a higher initial operating pressure. A higher value of the margin of error indicates the stochastic nature of hydrate formation. It is known that promoters reduce the probabilistic nature of gas hydrates. However, at lower concentrations or lower operating pressure, the effect of promoters becomes weaker. Therefore, additional experiments are required to reduce the margin of error in such cases.

3.6. Practical Implications

Table A11 in Appendix C summarizes recent studies on the use of histidine and methionine to promote CH_4 gas hydrates. In general, previous studies showed that histidine promoted the kinetics of CH_4 hydrate formation at a concentration (1000–10,000 ppm) such that the promotion effect increased with concentration and total gas uptake was similar to SDS at 10,000 ppm (in a stirred system) [37]. Histidine also showed a promoting effect at 273 K in an unstirred system at lower concentrations [36]. Veluswamy et al. [35] pointed out that the ability of histidine to promote the formation of CH_4 hydrates also depends on the concentration and that it starts to behave like an inhibitor at concentrations greater than 1 wt%. They also noticed that non-polar hydrophobic amino acids showed 5–10 times better promotion effect than polar hydrophilic amino acids. The inhibitory effect of histidine might be due to a charged side chain group that forms a van der Waals interaction and an electrostatic interaction with the surface of the hydrate crystal, blocking further nucleation [21]. Our recent publications showed that histidine did not promote CH_4 hydrate formation when tested in a rocking cell at temperatures greater than 273.15 K [21,50]. This

could be due to the difference in reactor design, sample volume, experiment type (constant volume vs. constant pressure), and mechanical agitation (rocking vs. stirring). We believe that rocking may be a more moderate form of mechanical agitation than stirring. In this study, histidine acted as a promoter when the temperature was reduced below 273.15 K; thus, the shortcoming of agitation was compensated for by the higher subcooling. In some similar studies, histidine was found to strongly inhibit the formation of CO_2 hydrate [55,56]. In another study, no improvement in formation kinetics was observed when guest molecules were replaced from CH_4 to CO_2/N_2 [30]. Such studies confirm that guest molecules also affect promotion and inhibition behavior. On the other hand, methionine shows an improvement in formation kinetics for both CH_4 and CO_2 gas hydrates, even under non-stirred conditions [20], and its promotion ability is similar to that of SDS [30,50].

Within the limited scope of the present study (methionine and histidine), we observed that the kinetics of CH_4 hydrate formation and total gas uptake in the presence of hydrophobic and hydrophilic amino acids are almost the same above a certain concentration at subzero temperatures. Available experimental studies on hydrate formation (above 0 °C) using different amino acids indicate different kinetics and formation characteristics (promoter, inhibitor, kinetics, thermodynamics) [26]. Therefore, a thorough study testing different amino acids at sub-zero temperatures is required. Amino acids as hydrate promoters are proposed to replace SDS, because SDS generates foam when the system is degassed, leading to additional operating costs [50,57]. Previous studies and this study indicate an additional advantage of using amino acids over SDS, as the self-preservation of CH_4 hydrate is significantly improved in the presence of amino acids compared to pure water and SDS. The tendency for self-preservation also differs between the bulk phase and the porous medium, as a porous medium increases the dissociation of total surface area, and the hydrate dissociation depends on the hydrate surface area of the hydrate [64,65]. The presence of a porous medium controls the hydrate morphology and the thermodynamics of the hydrate stability. The hydrate morphology controls the total hydrate surface area, while the pore size distribution controls the hydrate stability. The pore-scale visualization studies have shown that hydrate remained stable in narrow pore throats outside of their stability zone [6,66]. In another study, the correlation of the size of the hydrate particles with self-preservation was investigated and the particle particles larger than 0.5 mm in diameter showed a high degree of self-preservation [67]. The search for better chemicals that could improve formation kinetics and self-preservation and chemically influenced self-preservation correlation with the size of the hydrate particles and the porous medium is the subject of further investigation.

4. Conclusions

This study supports the experimental evidence for the use of amino acids as CH_4 hydrate stabilizers for natural gas storage and natural gas transportation. Amino acids are considered potential chemicals that can be used in the storage and transportation of natural gas in the form of hydrates, either as a standalone chemical or in combination with other thermodynamic promoters [41]. When used in low dosage, some of the amino acids act as promoters, and the promoter ability is related to the hydrophobic nature of amino acids. Such correlations were based on stirred/unstirred reactors and above 0 °C. Therefore, in this study, we investigated the ability to promote CH_4 hydrate and the subsequent tendency to self-preservation in the presence of hydrophobic, hydrophilic amino acids at T < 0 °C. We investigated the effect of the hydrophobicity of amino acids (AA) (hydrophilic and hydrophobic), concentration variation (100 ppm–20,000 ppm), pressure (60–120 bar) and temperature (1 °C and −2 °C) on the formation and self-preservation kinetics. The following are the main conclusions:

- At T > 0 °C, histidine showed a weaker promotion ability compared to methionine. Promotion ability improved slightly by increasing the pressure or concentration. Optimal gas uptake for methionine was observed at a concentration of 3000–10,000 ppm. The difference in hydrophobicity of the amino acids did not affect the dissociation tem-

perature of the hydrate, and the change in dissociation temperature was independent of the change in concentration;

- The ability to promote CH_4 hydrate in the presence of amino acids depends on concentration, reactor design, degree of mechanical agitation, and temperature. The influence of these parameters on the promotion ability is more evident for hydrophilic amino acids;
- The CH4 hydrate promotion abilities in the presence of histidine improved dramatically when the temperature dropped below 0 °C. L-methionine promoted the growth of CH_4 hydrate even with a lower driving force than histidine. Maximum gas uptake was measured at concentrations between 3000 and 10,000 ppm;
- The dissociation temperature of the CH_4 hydrate was independent of the type or concentration of amino acids;
- The ability of CH_4 hydrate to self-preserve is affected by the presence of amino acids and their concentration. An increase in amino acid concentration increases the metastability of CH_4 hydrate. Hydrophobic amino acids showed better metastability compared to hydrophilic amino acids. The effect of amino acids on metastability was more evident at a concentration of 10,000 ppm or greater.

Author Contributions: Conceptualization, methodology, investigation, project administration, supervision, original draft writing preparation and review and editing, Formal analysis, review & editing: J.S.P.; Investigation: S.K.; Supervision, project administration, and funding acquisition: N.v.S. All authors have read and agreed to the published version of the manuscript.

Funding: This research is funded by The Danish Council for Independent Research.

Institutional Review Board Statement: Not Applicable.

Informed Consent Statement: Not Applicable.

Data Availability Statement: Not Applicable.

Conflicts of Interest: The authors declare no conflict of interest.

Appendix A

Table A1. Shows T_{eq} (°C) for CH_4 hydrate calculated at different pressures using the CSMgem software. To (pure water) case is also mentioned.

PCH_4 (bar)	T_{eq} (°C)	T_o (Water) (Fresh)	T_o (Water) (Memory)
120	14.4	13.0	13.2
100	12.9	10.5 (90 bar)	10.8 (90 bar)
80	10.9	8.4 (70 bar)	8.6 (70 bar)
60	8.2	5.4 (50 bar)	5.5 (50 bar)

Table A2. Onset nucleation temperature T_0 (°C) (averaged) and Margin of error (ME) for L-histidine under different concentrations (100 ppm to 20,000 ppm).

	P = 120 bar		P = 100 bar	
Histidine (ppm)	T_0 (°C)	ME	T_0 (°C)	ME
100	10.7	0.4	11.4	0.9
1000	12.2	2.7	11.2	1.8
3000	12.3	-	11.3	-
10,000	11.7	-	11.5	0.9
20,000	12.4	0.4	11.2	2.7
MSE	0.23		0.01	

Table A3. Onset nucleation temperature T_0 (°C) (average) and ME for L-methionine at different concentrations. (100 ppm to 20,000 ppm).

	P = 100 bar		P = 80 bar		P = 60 bar	
Methionine (ppm)	**T_0 (°C)**	**ME**	**T_0 (°C)**	**ME**	**T_{011} (°C)**	**ME**
100	11.1	0.9	9.3	0.4	6.6	0.4
1000	11.2	0.9	9.3	0.9	6.5	0.4
3000	11.0	2.2	9.3	0.9	6.9	0.0
10,000	10.8	4.0	9.1	1.3	6.6	0.4
20,000	10.7	0.0	9.1	0.0	6.5	0.9
MSE	0.01		0.002		0.02	

Table A4. Information about the dissociation temperature T_d (°C) in the presence of L-methionine and L-histidine for different concentrations (100–20,000 ppm), ME is margin of error.

Chemical Type	**Methionine**						**Histidine**			
Concentration (in ppm)	**100 bar**	**ME**	**80 bar**	**ME**	**60 bar**	**ME**	**120 bar**	**ME**	**100 bar**	**ME**
100	13.1	0	11.1	0.9	8.4	0	14.7	0	13.1	0.4
1000	13.2	0	11.1	0	8.3	0	14.6	0	13.2	1.8
3000	13.1	0.4	10.9	0.4	8.4	0.45	14.6	0	13.1	0.9
10,000	13.1	0.4	11.0	0.4	8.4	0.45	14.6	0.4	13.1	0.4
20,000	13.0	0.4	10.9	0.4	8.2	0	14.5	0	13.0	0.4
MSE	0.002		0.005		0.005		0.001		0.002	

Table A5. Information on induction time (to) (in mins) in the presence of L-methionine and L-histidine for fresh and memory runs at different concentrations. NH indicates that there is no rapid hydrate formation.

Chemicals	**L-histidine**		**L-methionine**					
	P = 120 bar		**P= 100**		**P = 80 bar**		**P = 60 bar**	
Concentrations (ppm)	**Fresh**	**Memory**	**Fresh**	**Memory**	**Fresh**	**Memory**	**Fresh**	**Memory**
100	NH	NH	NH	NH	NH	NH	NH	NH
1000	NH	NH	4.5	7.8	4.3	8.0	5.5	12.3
3000	174	NH	2.8	6.0	2.8	6.5	4.0	8.0
10,000	142	114	1.3	4.0	1.8	4.0	2.8	4.3
20,000	6.5	12	<1	<1.1	<1.5	<1.6	<2.5	<2.6

Table A6. Information on total gas uptake in hydrates and pressure drop observed during the fresh and memory run in the presence of L-histidine at five different concentrations. (P1 = Initial starting pressure, ΔP = total pressure drop).

	Fresh Run		**Memory Run**	
	$nCH_4(H)$	**ΔP**	**$nCH_4(H)$**	**ΔP**
P1 = 100 bar				
100	0.014	6.9	0.009	4.6
1000	0.011	5.6	0.008	4.3

Table A6. *Cont.*

	Fresh Run		Memory Run	
	$nCH_4(H)$	**ΔP**	**$nCH_4(H)$**	**ΔP**
3000	0.014	6.9	0.011	5.5
10,000	0.011	5.6	0.008	4.1
20,000	0.012	6.1	0.011	5.4
MSE	0.0000086	1.4	0.00000152	0.28
P1 = 120 bar				
100	0.014	6.8	0.010	4.8
1000	0.011	5.4	0.009	4.4
3000	0.033	16.6	0.010	4.8
10,000	0.043	21.5	0.048	23.9
20,000	0.042	20.9	0.020	10.1
MSE	0.00031	7.9	0.00015	37.5

Table A7. Total gas uptake in hydrates and pressure drop during the fresh and memory run in the presence of L-methionine at five different concentrations. T = 1 °C, Peq = 28.68 bar ($nCH_4(H)$ = total moles of CH_4 stored in hydrates, ΔP = total pressure drop) * Single experiment details available only. ME = margin of error.

	Fresh			Memory		
	$\Delta nCH_4(H)$ (mol)	**ME**	**ΔP**	**$\Delta nCH_4(H)$ (mol)**	**ME**	**ΔP**
P1 = 60 bar						
100	0.015	0.002	8.8	0.009	0.001	5.5
1000	0.052	0.004	31.7	0.045	0.004	28.0
3000	0.053	0.003	32.3	0.046	0.005	28.6
10,000	0.050	0.008	30.4	0.044	0.000	27.0
20,000	0.052	0.003	31.7	0.045	0.004	28.0
MSE	0.00011		43.4	0.00065		41.8
P1 = 80 bar						
100	0.014	0.001	7.4	0.008	0.004	4.5
1000	0.072	0.003	41.3	0.041	0.038	22.6
3000	0.071	0.008	40.3	0.066	0.001	38.0
10,000	0.064	0.001	35.8	0.059	0.009	33.6
20,000 *	0.063	-	35.1	0.054	-	30.7
MSE	0.0003		107.1	0.00147		59.12
P1 = 100 bar						
100	0.012	0.002	6.2	0.007	0.004	3.3
1000	0.072	0.014	37.6	0.064	0.024	33.9
3000	0.069	0.001	36.3	0.065	0.007	34.5
10,000	0.065	0.000	33.9	0.060	0.008	31.5
20,000 *	0.063	-	32.8	0.056	-	29.1
MSE	0.0013		80.0	0.00124		89.3

Table A8. Total mole of CH_4 released in the presence of histidine at T = −2 °C. $\Delta nCH_4(H)$ is moles of CH_4 stored in hydrate at T = 1 °C. $nCH_4(Hb)$ is moles of CH_4 stored in hydrate at T = −2°C. ΔnCH_4 (R) is the moles of CH_4 release. R is the ratio of mole released/mole stored in hydrate with in 24 h.

	100 bar				120 bar			
Conc (ppm)	**$\Delta nCH_4(H)$**	**$\Delta nCH_4(Hb)$**	**$\Delta nCH_4(R)$**	**R**	**$\Delta nCH_4(H)$**	**$\Delta nCH_4(Hb)$**	**$\Delta nCH_4(R)$**	**R**
100	0.009	0.018	0.010	58%	0.010	0.015	0.013	89%
1000	0.008	0.056	0.031	56%	0.009	0.027	0.021	78%
3000	0.011	0.057	0.022	38%	0.010	0.058	0.014	24%
10,000	0.008	0.048	0.017	36%	0.048	0.119	0.028	23%
20,000	0.011	0.045	0.006	13%	0.020	0.048	0.005	10%
MSE	0.00000152	0.000158	0.000068		0.000151	0.000835	0.000059	

Table A9. Total mole CH_4 released in the presence of methionine at T = −2 °C. ΔnCH_4 (Hb) is the moles of CH_4 stored in hydrate at T = −2 °C. ΔnCH_4 (R) is moles of CH_4 release. Thus, R is the ratio of mole released/mole stored in hydrate in 24 h. (Second run).

		T > 0 °C	**T < 0 °C**	**T < 0 °C**	
Pressure	**Concentration**	**$\Delta nCH_4(H)$**	**$\Delta nCH_4(Hb)$**	**$\Delta nCH_4(Re)$**	**R**
60 bar	100	0.009	0.019	0.003	13%
	1000	0.045	0.056	0.017	30%
	3000	0.045	0.057	0.012	21%
	10,000	0.044	0.053	0.007	12%
	20,000	0.045	0.049	0.002	3%
	MSE	0.000104	0.000136	0.0000289	
80 bar	100	0.009	0.012	0.002	17%
	1000	0.035	0.064	0.034	53%
	3000	0.066	0.067	0.022	34%
	10,000	0.058	0.058	0.009	15%
	20,000	0.054	0.055	0.003	6%
	MSE	0.00016	0.00084	0.00014	
100 bar	100	0.006	0.008	0.003	34%
	1000	0.060	0.060	0.034	56%
	3000	0.064	0.066	0.028	42%
	10,000	0.059	0.059	0.011	19%
	20,000	0.056	0.056	0.004	7%
	MSE	0.000273	0.00085	0.000192	

Table A10. Total mole CH_4 released (average from two experiments) in the presence of methionine at T = −2 °C. ΔnCH_4 (Hb average) is the moles of CH_4 stored in hydrate at T = −2 °C. ΔnCH_4 (R) (average) is moles of CH_4 release. Thus, R (average) is the ratio of mole released/mole stored in hydrate in 24 h. SD is standard deviation. * reported value for single experiment.

Pressure	**Concentration**	**$\Delta nCH_4(Hb)$**	**ME**	**$\Delta nCH_4(Re)$**	**ME**	**R**
60 bar	100	0.018	0.004	0.009	-	47%
	1000	0.057	0.005	0.018	-	31%
	3000	0.058	0.006	0.022	-	38%
	10,000	0.054	0.007	0.018	-	33%
	20,000	0.050	0.007	0.012	-	24%

Table A10. *Cont.*

Pressure	Concentration	ΔnCH_4(Hb)	ME	ΔnCH_4(Re)	ME	R
	MSE	0.000149		0.000342		
80 bar	100	0.020	0.005	0.002	-	12%
	1000	0.067	0.023	0.032	0.013	47%
	3000	0.069	0.013	0.021	0.009	30%
	10,000	0.062	0.025	0.010	0.004	16%
	20,000 *	0.055	-	0.003	-	6%
	MSE	0.000238		0.000123		
100 bar	100	0.009	0.003	0.003	-	29%
	1000	0.064	0.025	0.034	-	52%
	3000	0.066	0.006	0.027	0.004	40%
	10,000	0.061	0.008	0.010	0.004	17%
	20,000 *	0.056	0.004	0.004	0.040	7%
	MSE	0.000291		0.000149		

Appendix B

Appendix B.1 Experimental Data Processing

The pressure change during the constant ramping experiment is shown in Figures 2 and 3 for L-methionine and L-histidine, respectively. During constant ramping, an initial pressure reduction is observed due to a decrease in temperature and CH_4 solubility. The onset nucleation temperature T_o is identified as the temperature at the start of hydrate nucleation when the first macroscopic detection of hydrate formation occurs before rapid hydrate formation [68]. It is also possible that nucleation may have occurred earlier but could not be detected due to a lack of visual observation.

The subcooling temperature (ΔT_{sub}) is calculated as the difference between T_{eq} and the operating temperature T_o [69]. T_{eq} is calculated using the CSMGem software while T_{op} is the operating temperature usually referred to as the temperature during the isothermal test [70].

$$\Delta T_{sub,iso} = T_{eq} - T_{op}. \quad \text{(A1)}$$

The subcooling measurement explains the effect of concentration on the driving force and growth profile. As explained above, T_o is the temperature at which hydrate nucleation starts during constant-temperature ramping. T_o correlate the effect of driving force on the hydrate growth curve. The subcooling requirement during constant ramping can be expressed as:

$$\Delta T_{sub,cons} = T_{eq} - T_o. \quad \text{(A2)}$$

$\Delta T_{sub,cons} - \Delta T_{sub,iso}$ gives the difference between the operating temperature (isothermal tests) and the expected onset temperature [71]. It is calculated by:

$$\Delta T_{sub,cons} - \Delta T_{sub,iso} = (T_{eq} - T_o) - (T_{eq} - T_{op}) = T_{op} - T_o. \quad \text{(A3)}$$

T_{eq} is dependent on initial operating conditions for a given solution. $T_{op} > T_o$ indicates immediate hydrate formation, while $T_{op} < T_o$ indicates delayed hydrate formation. In the presence of promoters, subcooling measurement can provide an effect of concentration on hydrate nucleation.

The induction time (t_o) is defined as the time from the start of the rocking to a first significant drop in pressure, as proposed in [48]. The pressure curve in the pressure-time data in isothermal experiments is also used to calculate the total gas uptake.

The total number of moles of CH_4 injected into the pressure cell is calculated is given by (A4)

$$nCH_{4,T} = \frac{P_1 V}{Z_1 RT}. \quad (A4)$$

P_1 is the initial operating pressure after CH_4 gas is injected into the high-pressure cell, where $V(V = V_T - V_L)$ is the available gas volume in the reactor. V_T is the total cell volume and V_L is the solution volume (equal to 10 mL). T is the temperature of the isothermal test. The compressibility factor Z_1 at a given pressure and temperature is calculated using the Benedict-Webb-Rubin-Starling equation of state. R is the universal gas constant, 8.314 $J{\cdot}mol^{-1}{\cdot}K^{-1}$. Under the constant-volume assumption, a mole of CH_4, $n_{CH_{4,H}}$ in residual gas after hydrate is given by Equation (A5):

$$n_{CH_{4,H}} = \frac{P_2 V}{Z_2 RT}, \quad (A5)$$

where P_2 is the pressure at the end of isothermal, and Z_2 is the compressibility factor corresponding to P_2, T. The change in the total number of moles of CH_4, $\Delta n_{CH4,H}$, also known as total gas uptake at the end of CH_4 hydrate formation, is given by:

$$\Delta n_{CH4,H} = \frac{P_1 V}{Z_1 RT} - \frac{P_2 V}{Z_2 RT}. \quad (A6)$$

Appendix C

Table A11. Summary of similar studies carried out with L-methionine and L-histidine for CH_4 gas hydrates.

S. No	Proposed Role	Conc.		Experimental Conditions	Key Results
Methionine					
1.1	KHP	0.5 wt%	[20]	P = 33–53 bar, T = 273–275 K, non-stirred conditions	L-methionine shows efficient promotion for CH_4 hydrates.
1.2	KHP	0.5 wt%	[36]	P = 95 bar, T = 273 K, non-stirred.	Able to promote hydrate formation kinetics with decreasing stability.
Histidine					
2.1	KHP	0.1, 1 wt%	[37]	P = 50 bar, T= 274.15 K, Stirred = 150 rpm	Show promotion effect and increase with concentration increase, reduce induction time compared to water, but slower gas uptake than 1 wt% SDS.
2.2	KHP	0.3 and 1 wt%	[35]	P = 100 bar, T = 275.2 K, stirred and unstirred reactor. Stirred = 500 rpm	Histidine shows a similar gas uptake profile in stirred and unstirred reactor. At 1 wt%, the promotion rate for CH_4 hydrate is 2–3 times greater than at a concentration of 0.3 wt%.
2.3	KHP	0.5 wt%	[36]	P = 95 bar, T = 273 K, non-stirred.	Able to promote hydrate formation kinetics with decreasing stability.
2.4	KHI	1 wt%	[21]	P = 24.5 bar, T = 275.15 K	The mixture of CH_4 + C_3H_8 was tested using different impeller systems. Histidine was shown to behave as a kinetic inhibitor in terms of hydrate growth rate.

References

1. Ibrahim, I.A.; Ötvös, T.; Gilmanova, A.; Rocca, E.; Ghanem, C.; Wanat, M. *International Energy Agency*; Kluwer Law International BV: Alphen aan den Rijn, ZUID-HOLLAND, The Netherlands, 2021; ISBN 9403529539.
2. Veluswamy, H.P.; Kumar, A.; Seo, Y.; Lee, J.D.; Linga, P. A review of solidified natural gas (SNG) technology for gas storage via clathrate hydrates. *Appl. Energy* **2018**, *216*, 262–285. [CrossRef]

3. Sadeq, D.; Iglauer, S.; Lebedev, M.; Smith, C.; Barifcani, A. Experimental determination of hydrate phase equilibrium for different gas mixtures containing methane, carbon dioxide and nitrogen with motor current measurements. *J. Nat. Gas Sci. Eng.* **2017**, *38*, 59–73. [CrossRef]
4. Pandey, J.S.; Ouyang, Q.; Solms, N. von New insights into the dissociation of mixed CH_4/CO_2 hydrates for CH4 production and CO_2 storage. *Chem. Eng. J.* **2022**, *427*, 131915. [CrossRef]
5. Pandey, J.S.; Karantonidis, C.; Ouyang, Q.; von Solms, N. Cyclic Depressurization-Driven Enhanced CH4 Recovery after CH_4–CO_2 Hydrate Swapping. *Energy Fuels* **2021**, *35*, 9521–9537. [CrossRef]
6. Pandey, J.S.; Almenningen, S.; von Solms, N.; Ersland, G. Pore-Scale Visualization of CH_4 Gas Hydrate Dissociation under Permafrost Conditions. *Energy Fuel* **2021**, *35*, 1178–1196. [CrossRef]
7. Pan, Z.; Liu, Z.; Zhang, Z.; Shang, L.; Ma, S. Effect of silica sand size and saturation on methane hydrate formation in the presence of SDS. *J. Nat. Gas Sci. Eng.* **2018**, *56*, 266–280. [CrossRef]
8. Chong, Z.R.; Yang, S.H.B.; Babu, P.; Linga, P.; Li, X. Sen Review of natural gas hydrates as an energy resource: Prospects and challenges. *Appl. Energy* **2016**, *162*, 1633–1652. [CrossRef]
9. Pandey, J.; Solms, N. Hydrate Stability and Methane Recovery from Gas Hydrate through CH_4–CO_2 Replacement in Different Mass Transfer Scenarios. *Energies* **2019**, *12*, 2309. [CrossRef]
10. Brown, T.D.; Taylor, C.E.; Bernardo, M.P. Rapid Gas Hydrate Formation Processes: Will They Work? *Energies* **2010**, *3*, 1154–1175. [CrossRef]
11. Sadeq, D.; Alef, K.; Iglauer, S.; Lebedev, M.; Barifcani, A. Compressional wave velocity of hydrate-bearing bentheimer sediments with varying pore fillings. *Int. J. Hydrog. Energy* **2018**, *43*, 23193–23200. [CrossRef]
12. Okutani, K.; Kuwabara, Y.; Mori, Y.H. Surfactant effects on hydrate formation in an unstirred gas / liquid system: An experimental study using methane and sodium alkyl sulfates. *Chem. Eng. Sci.* **2008**, *63*, 183–194. [CrossRef]
13. Zhong, Y.; Rogers, R.E. Surfactant effects on gas hydrate formation. *Chem. Eng. Sci.* **2000**, *55*, 4175–4187. [CrossRef]
14. Mimachi, H.; Takahashi, M.; Takeya, S.; Gotoh, Y.; Yoneyama, A.; Hyodo, K.; Takeda, T.; Murayama, T. Effect of Long-Term Storage and Thermal History on the Gas Content of Natural Gas Hydrate Pellets under Ambient Pressure. *Energy Fuels* **2015**, *29*, 4827–4834. [CrossRef]
15. Zhang, G.; Rogers, R.E. Ultra-stability of gas hydrates at 1 atm and 268.2 K. *Chem. Eng. Sci.* **2008**, *63*, 2066–2074. [CrossRef]
16. Hachikubo, A.; Takeya, S.; Chuvilin, E.; Istomin, V. Preservation phenomena of methane hydrate in pore spaces. *Phys. Chem. Chem. Phys.* **2011**, *13*, 17449. [CrossRef]
17. Mel'nikov, V.P.; Podenko, L.S.; Nesterov, A.N.; Drachuk, A.O.; Molokitina, N.S.; Reshetnikov, A.M. Self-preservation of methane hydrates produced in "dry water". *Dokl. Chem.* **2016**, *466*, 53–56. [CrossRef]
18. Sato, H.; Sakamoto, H.; Ogino, S.; Mimachi, H.; Kinoshita, T.; Iwasaki, T.; Sano, K.; Ohgaki, K. Self-preservation of methane hydrate revealed immediately below the eutectic temperature of the mother electrolyte solution. *Chem. Eng. Sci.* **2013**, *91*, 86–89. [CrossRef]
19. Takeya, S.; Mimachi, H.; Murayama, T. Methane storage in water frameworks: Self-preservation of methane hydrate pellets formed from NaCl solutions. *Appl. Energy* **2018**, *230*, 86–93. [CrossRef]
20. Prasad, P.S.R.; Sai Kiran, B. Clathrate Hydrates of Greenhouse Gases in the Presence of Natural Amino Acids: Storage, Transportation and Separation Applications. *Sci. Rep.* **2018**, *8*, 8560. [CrossRef]
21. Pandey, J.S.; Daas, Y.J.; von Solms, N. Methane hydrate formation, storage and dissociation behavior in unconsolidated sediments in the presence of environment-friendly promoters. In Proceedings of the SPE Europec Conference, Virtual, 1–3 December 2020.
22. Bai, D.; Zhang, D.; Zhang, X.; Chen, G. Origin of Self-preservation Effect for Hydrate Decomposition: Coupling of Mass and Heat Transfer Resistances. *Sci. Rep.* **2015**, *5*, 1–13. [CrossRef] [PubMed]
23. Schramm, L.L.; Stasiuk, E.N.; Marangoni, D.G. Surfactants and their applications. *Annu. Rep. Prog. Chem.-Sect. C* **2003**, *99*, 3–48. [CrossRef]
24. Zhang, J.S.; Lee, S.; Lee, J.W. Solubility of sodium dodecyl sulfate near propane and carbon dioxide hydrate-forming conditions. *J. Chem. Eng. Data* **2007**, *52*, 2480–2483. [CrossRef]
25. Demissie, H.; Duraisamy, R. Effects of electrolytes on the surface and micellar characteristics of Sodium dodecyl sulphate surfactant solution. *J. Sci. Innov. Res.* **2016**, *5*, 208–214.
26. Lal, B.; Mukhtar, H.; Bavoh, C.B.; Osei, H.; Sabil, K.M.; Lal, B.; Osei, H.; Sabil, K.M.; Mukhtar, H.; Bavoh, C.B.; et al. A Review on the Role of Amino Acids in Gas Hydrate Inhibition, CO_2 Capture and Sequestration, and Natural Gas Storage. *J. Nat. Gas Sci. Eng.* **2019**, *64*, 52–71.
27. Nasir, Q.; Suleman, H.; Elsheikh, Y.A. A review on the role and impact of various additives as promoters/ inhibitors for gas hydrate formation. *J. Nat. Gas Sci. Eng.* **2020**, *76*, 103211. [CrossRef]
28. Prasad, P.S.R.; Kiran, B.S. Are the amino acids thermodynamic inhibitors or kinetic promoters for carbon dioxide hydrates? *J. Nat. Gas Sci. Eng.* **2018**, *52*, 461–466. [CrossRef]
29. Kyte, J.; Doolittle, R.F. A simple method for displaying the hydropathic character of a protein. *J. Mol. Biol.* **1982**, *157*, 105–132. [CrossRef]
30. Pandey, J.S.; Daas, Y.J.; von Solms, N. Screening of amino acids and surfactant as hydrate promoter for CO_2 capture from flue gas. *Processes* **2020**, *8*, 124. [CrossRef]

31. Sa, J.H.; Kwak, G.H.; Han, K.; Ahn, D.; Lee, K.H. Gas hydrate inhibition by perturbation of liquid water structure. *Sci. Rep.* **2015**, *5*, 1–9. [CrossRef] [PubMed]
32. Ide, M.; Maeda, Y.; Kitano, H. Effect of hydrophobicity of amino acids on the structure of water. *J. Phys. Chem. B* **1997**, *101*, 7022–7026. [CrossRef]
33. Sa, J.H.; Kwak, G.H.; Lee, B.R.; Park, D.H.; Han, K.; Lee, K.H. Hydrophobic amino acids as a new class of kinetic inhibitors for gas hydrate formation. *Sci. Rep.* **2013**, *3*, 1–7. [CrossRef] [PubMed]
34. Alireza Bagherzadeh, S.; Alavi, S.; Ripmeester, J.A.; Englezos, P. Why ice-binding type i antifreeze protein acts as a gas hydrate crystal inhibitor. *Phys. Chem. Chem. Phys.* **2015**, *17*, 9984–9990. [CrossRef] [PubMed]
35. Veluswamy, H.P.; Lee, P.Y.; Premasinghe, K.; Linga, P. Effect of Biofriendly Amino Acids on the Kinetics of Methane Hydrate Formation and Dissociation. *Ind. Eng. Chem. Res.* **2017**, *56*, 6145–6154. [CrossRef]
36. Liu, Y.; Chen, B.; Chen, Y.; Zhang, S.; Guo, W.; Cai, Y.; Tan, B.; Wang, W. Methane Storage in a Hydrated Form as Promoted by Leucines for Possible Application to Natural Gas Transportation and Storage. *Energy Technol.* **2015**, *3*, 815–819. [CrossRef]
37. Bhattacharjee, G.; Choudhary, N.; Kumar, A.; Chakrabarty, S.; Kumar, R. Effect of the amino acid L-histidine on methane hydrate growth kinetics. *J. Nat. Gas Sci. Eng.* **2016**, *35*, 1453–1462. [CrossRef]
38. Borchardt, L.; Casco, M.E.; Silvestre-Albero, J. Methane Hydrate in Confined Spaces: An Alternative Storage System. *ChemPhysChem* **2018**, *19*, 1298–1314. [CrossRef]
39. Takeya, S.; Ripmeester, J.A. Dissociation behavior of clathrate hydrates to ice and dependence on guest molecules. *Angew. Chemie-Int. Ed.* **2008**, *47*, 1276–1279. [CrossRef] [PubMed]
40. Falenty, A.; Kuhs, W.F.; Glockzin, M.; Rehder, G. "self-preservation" of CH_4 hydrates for gas transport technology: Pressure-temperature dependence and ice microstructures. *Energy Fuels* **2014**, *28*, 6275–6283. [CrossRef]
41. Bhattacharjee, G.; Goh, M.N.; Arumuganainar, S.E.K.K.; Zhang, Y.; Linga, P. Ultra-rapid uptake and the highly stable storage of methane as combustible ice. *Energy Environ. Sci.* **2020**, *13*, 4946–4961. [CrossRef]
42. Sato, H.; Tsuji, T.; Nakamura, T.; Uesugi, K.; Kinoshita, T.; Takahashi, M.; Mimachi, H.; Iwasaki, T.; Ohgaki, K. Preservation of Methane Hydrates Prepared from Dilute Electrolyte Solutions. *Int. J. Chem. Eng.* **2009**, *2009*, 843274. [CrossRef]
43. Mimachi, H.; Takeya, S.; Gotoh, Y.; Yoneyama, A.; Hyodo, K.; Takeda, T.; Murayama, T. Dissociation behaviors of methane hydrate formed from NaCl solutions. *Fluid Phase Equilib.* **2016**, *413*, 22–27. [CrossRef]
44. Chen, X.; Li, S.; Zhang, P.; Chen, W.; Wu, Q.; Zhan, J.; Wang, Y. Promoted Disappearance of CO_2 Hydrate Self-Preservation Effect by Surfactant SDS. *Energies* **2021**, *14*, 3909. [CrossRef]
45. Ohno, H.; Narita, H.; Nagao, J. Different Modes of Gas Hydrate Dissociation to Ice Observed by Microfocus X-ray Computed Tomography. *J. Phys. Chem. Lett.* **2011**, *2*, 201–205. [CrossRef]
46. Naeiji, P.; Varaminian, F. Differential scanning calorimetry measurements and modeling of methane + THF hydrate growth kinetics based on non-equilibrium thermodynamics. *J. Mol. Liq.* **2018**, *263*, 22–30. [CrossRef]
47. Mcnamee, K.P. *Evaluation of Kinetic Hydrate Inhibitor Performance by High-Pressure Differential Scanning Calorimetry*; Offshore Technology Conference: Houston, TX, USA, 2011.
48. Lone, A.; Kelland, M.A. Exploring kinetic hydrate inhibitor test methods and conditions using a multicell steel rocker rig. *Energy Fuels* **2013**, *27*, 2536–2547. [CrossRef]
49. Sa, J.-H.; Melchuna, A.; Zhang, X.; Morales, R.E.M.; Cameirão, A.; Herri, J.-M.; Sum, A.K. Rock-Flow Cell: An Innovative Benchtop Testing Tool for Flow Assurance Studies. *Ind. Eng. Chem. Res.* **2019**, *58*, 8544–8552. [CrossRef]
50. Shanker Pandey, J.; Jouljamal Daas, Y.; Paul Karcz, A.; von Solms, N. Methane Hydrate Formation Behavior in the Presence of Selected Amino Acids. *J. Phys. Conf. Ser.* **2020**, *1580*, 012003. [CrossRef]
51. Pandey, J.S.; Daas, Y.J.; Karcz, A.P.; von Solms, N. Enhanced Hydrate-Based Geological CO_2 Capture and Sequestration as a Mitigation Strategy to Address Climate Change. *Energies* **2020**, *13*, 5661. [CrossRef]
52. Qureshi, M.F.; Khraisheh, M.; Almomani, F. Doping amino acids with classical gas hydrate inhibitors to facilitate the hydrate inhibition effect at low dosages. *Greenh. Gases Sci. Technol.* **2020**, *10*, 783–794. [CrossRef]
53. Bell, S. *Good Practice Guide No. 11—Introductory Guide to Uncertainty of Measurement*; National Physical Laboratory: Teddington, UK, 2001; p. 41.
54. Daraboina, N.; Pachitsas, S.; von Solms, N. Experimental validation of kinetic inhibitor strength on natural gas hydrate nucleation. *Fuel* **2015**, *139*, 554–560. [CrossRef]
55. Daraboina, N.; von Solms, N. The combined effect of thermodynamic promoters tetrahydrofuran and cyclopentane on the kinetics of flue gas hydrate formation. *J. Chem. Eng. Data* **2015**, *60*, 247–251. [CrossRef]
56. Qureshi, M.F.; Atilhan, M.; Altamash, T.; Tariq, M.; Khraisheh, M.; Aparicio, S.; Tohidi, B. Gas Hydrate Prevention and Flow Assurance by Using Mixtures of Ionic Liquids and Synergent Compounds: Combined Kinetics and Thermodynamic Approach. *Energy Fuels* **2016**, *30*, 3541–3548. [CrossRef]
57. Pandey, J.S.; Daas, Y.J.; von Solms, N. Insights into Kinetics of Methane Hydrate Formation in the Presence of Surfactants. *Processes* **2019**, *7*, 598. [CrossRef]
58. Mu, L.; von Solms, N. Inhibition of natural gas hydrate in the system containing salts and crude oil. *J. Pet. Sci. Eng.* **2020**, *188*, 106940. [CrossRef]
59. Lee, D.; Go, W.; Seo, Y. Experimental and computational investigation of methane hydrate inhibition in the presence of amino acids and ionic liquids. *Energy* **2019**, *182*, 632–640. [CrossRef]

60. Roosta, H.; Dashti, A.; Mazloumi, S.H.; Varaminian, F. The dual effect of amino acids on the nucleation and growth rate of gas hydrate in ethane + water, methane + propane + water and methane + THF + water systems. *Fuel* **2018**, *212*, 151–161. [CrossRef]
61. Longinos, S.N.; Parlaktuna, M. Kinetic study of the effect of amino acids on methane (95%)–propane (5%) hydrate formation. *React. Kinet. Mech. Catal.* **2021**, *133*, 753–763. [CrossRef]
62. Jensen, L.; Thomsen, K.; von Solms, N.; Wierzchowski, S.; Walsh, M.R.; Koh, C.A.; Sloan, E.D.; Wu, D.T.; Sum, A.K. Calculation of liquid water-hydrate-methane vapor phase equilibria from molecular simulations. *J. Phys. Chem. B* **2010**, *114*, 5775–5782. [CrossRef]
63. Koh, C.A.; Sloan, E.D.; Sum, A.K.; Wu, D.T. Fundamentals and applications of gas hydrates. *Annu. Rev. Chem. Biomol. Eng.* **2011**, *2*, 237–257. [CrossRef]
64. Longinos, S.N.; Parlaktuna, M. Are the amino acids inhibitors or promoters on methane (95%)–propane (5%) hydrate formation? *React. Kinet. Mech. Catal.* **2021**, *132*, 795–809. [CrossRef]
65. Chen, X.; Espinoza, D.N. Surface area controls gas hydrate dissociation kinetics in porous media. *Fuel* **2018**, *234*, 358–363. [CrossRef]
66. Pandey, J.S.; Strand, Ø.; von Solms, N.; Ersland, G.; Almenningen, S. Direct Visualization of CH_4/CO_2 Hydrate Phase Transitions in Sandstone Pores. *Cryst. Growth Des.* **2021**, *21*, 2793–2806. [CrossRef]
67. Mimachi, H.; Takeya, S.; Yoneyama, A.; Hyodo, K.; Takeda, T.; Gotoh, Y.; Murayama, T. Natural gas storage and transportation within gas hydrate of smaller particle: Size dependence of self-preservation phenomenon of natural gas hydrate. *Chem. Eng. Sci.* **2014**, *118*, 208–213. [CrossRef]
68. Kelland, M.A.; Abrahamsen, E.; Ajiro, H.; Akashi, M. Kinetic Hydrate Inhibition with N-Alkyl-N-vinylformamide Polymers: Comparison of Polymers to n-Propyl and Isopropyl Groups. *Energy Fuels* **2015**, *29*, 4941–4946. [CrossRef]
69. Kelland, M.A. History of the development of low dosage hydrate inhibitors. *Energy Fuels* **2006**, *20*, 825–847. [CrossRef]
70. Sloan, E.D., Jr.; Koh, C.A.; Koh, C.A. *Clathrate Hydrates of Natural Gases*, 3rd ed.; CRC Press: Boca Raton, FL, USA, 2007; ISBN 9780429129148.
71. Sloan, E.D.; Subramanian, S.; Matthews, P.N.; Lederhos, J.P.; Khokhar, A.A. Quantifying hydrate formation and kinetic inhibition. *Ind. Eng. Chem. Res.* **1998**, *37*, 3124–3132. [CrossRef]